Bioactive Materials 39 (2024) 255–272

Contents lists available at ScienceDirect

Bioactive Materials

journal homepage: www.keaipublishing.com/en/journals/bioactive-materials

Intra-articular sustained-release of pirfenidone as a disease-modifying treatment for early osteoarthritis

Xiaobo Zhu [a,c,d,f], Mingde Cao [a,c,d], Kejia Li [a,d], Yau-Tsz Chan [a,b,d], Hon-Fai Chan [a,b], Yi-Wah Mak [a,b], Hao Yao [c,f], Jing Sun [a,d], Michael Tim-Yun Ong [c,d], Kevin Ki-Wai Ho [c], Chien-Wei Lee [a,b], Oscar Kuang-Sheng Lee [a,c], Patrick Shu-Hang Yung [a,c,d], Yangzi Jiang [a,b,c,d,e,*]

[a] *Institute for Tissue Engineering and Regenerative Medicine, School of Biomedical Sciences, Faculty of Medicine, The Chinese University of Hong Kong, Shatin, Hong Kong Special Administrative Region of China*
[b] *School of Biomedical Sciences, Faculty of Medicine, The Chinese University of Hong Kong, Shatin, Hong Kong Special Administrative Region of China*
[c] *Department of Orthopaedics & Traumatology, Faculty of Medicine, The Chinese University of Hong Kong, Prince of Wales Hospital, Shatin, Hong Kong Special Administrative Region of China*
[d] *Center for Neuromusculoskeletal Restorative Medicine, Hong Kong Special Administrative Region of China*
[e] *Key Laboratory for Regenerative Medicine, Ministry of Education, School of Biomedical Sciences, Faculty of Medicine, The Chinese University of Hong Kong, Hong Kong Special Administrative Region of China*
[f] *Department of Orthopaedic Surgery, The First Affiliated Hospital, School of Medicine, Zhejiang University, China*

ARTICLE INFO

Keywords:
TGFβ1 signaling
Osteoarthritis
Subchondral bone
Pirfenidone
DMOAD

ABSTRACT

Osteoarthritis (OA) is a major clinical challenge, and effective disease-modifying drugs for OA are still lacking due to the complicated pathology and scattered treatment targets. Effective early treatments are urgently needed to prevent OA progression. The excessive amount of transforming growth factor β (TGFβ) is one of the major causes of synovial fibrosis and subchondral bone sclerosis, and such pathogenic changes in early OA precede cartilage damage. Herein we report a novel strategy of intra-articular sustained-release of pirfenidone (PFD), a clinically-approved TGFβ inhibitor, to achieve disease-modifying effects on early OA joints. We found that PFD effectively restored the mineralization in the presence of excessive amount of TGFβ1 (as those levels found in patients' synovial fluid). A monthly injection strategy was then designed of using poly lactic-*co*-glycolic acid (PLGA) microparticles and hyaluronic acid (HA) solution to enable a sustained release of PFD (the "PLGA-PFD + HA" strategy). This strategy effectively regulated OA progression in destabilization of the medial meniscus (DMM)- induced OA mice model, including preventing subchondral bone loss in early OA and subchondral bone sclerosis in late OA, and reduced synovitis and pain with cartilage preservation effects. This finding suggests the promising clinical application of PFD as a novel disease-modifying OA drug.

1. Data availability statement

The data that support the findings of this study are available from the corresponding author upon reasonable request.

Funding statement

The project was supported by (1) the National Key R&D Program of China (Project No. 2019YFA0111900 to YJ), which is financed by the Ministry of Science and Technology of the People's Republic of China (MOST, China); (2) this work described in this paper was partially supported by a grant from the NSFC/RGC Joint Research Scheme

Peer review under responsibility of KeAi Communications Co., Ltd.
* Corresponding author. Institute for Tissue Engineering and Regenerative Medicine, School of Biomedical Sciences, Faculty of Medicine, The Chinese University of Hong Kong, Shatin, Hong Kong Special Administrative Region of China.
E-mail addresses: shawnzhu_ortho@zju.edu.cn (X. Zhu), mingdecao@link.cuhk.edu.hk (M. Cao), kejiali@cuhk.edu.hk (K. Li), helenchan@link.cuhk.edu.hk (Y.-T. Chan), honfaichan@cuhk.edu.hk (H.-F. Chan), yiwahmak@yahoo.com (Y.-W. Mak), yaohao@link.cuhk.edu.hk (H. Yao), jingsun@cuhk.edu.hk (J. Sun), michael.ong@cuhk.edu.hk (M.T.-Y. Ong), kevinho@cuhk.edu.hk (K.K.-W. Ho), icehikki@gmail.com (C.-W. Lee), oscarlee9203@gmail.com (O.K.-S. Lee), patrickyung@cuhk.edu.hk (P.S.-H. Yung), yangzjiang21@cuhk.edu.hk (Y. Jiang).

https://doi.org/10.1016/j.bioactmat.2024.05.028
Received 6 February 2024; Received in revised form 28 April 2024; Accepted 14 May 2024

sponsored by the Research Grants Council of the Hong Kong Special Administrative Region, China and the National Natural Science Foundation of China (Project No. N_CUHK483/22 to YJ); (3) the Center for Neuromusculoskeletal Restorative Medicine [CNRM at InnoHK, to YJ, HC, PY] by Innovation and Technology Commission (ITC) of Hong Kong SAR, China; (4) the Natural Science Foundation of China (Project No. 82302728 to XZ); (5) The Chinese University of Hong Kong.

2. Introduction

Osteoarthritis (OA) is the most prevalent joint disorder and the leading cause of disability worldwide [1,2]. The current clinical conservative management of OA includes primary oral administration of nonsteroidal anti-inflammatory drugs (NSAIDs) and intra-articular (I.A.) injection of hyaluronic acid (HA), a natural component of glycosaminoglycan in joints [3,4]. I.A. injection of HA can promote shock absorption, joint lubrication and proteoglycan synthesis and provide anti-inflammatory and chondroprotective effect, and is the second line of treatment for patients unresponsive to NSAIDs; however, this treatment is conditionally recommended by the Osteoarthritis Research Society International (OARSI) 2019 guideline for knee OA therapy [4] due to its high administration frequency, and short-term and limited therapeutic effects [5–7]. Effective disease-modifying OA drugs (DMOADs) are still under development, especially for the management of early OA stages.

The transforming growth factor β (TGFβ) superfamily members are crucial pleiotropic components involved in regulating joint homeostasis, including that of synovial tissue, cartilage and bone [8]. Several human-based studies have identified subchondral bone as a therapeutic target in early OA [9,10]. Abnormal subchondral bone remodeling is one of the main phenotypic features of early OA pathology preceding cartilage degeneration, which is initiated by overactivated osteoclast-induced bone resorption and the subsequent release of embedded bone active factors from the bone extracellular matrix, especially TGFβ. During bone remodeling, large amounts of active TGFβ are released from the bone matrix, which is a TGFβ reservoir (TGFβ1: 188 ng/g; TGFβ2: 14 ng/g, wet weight from fresh bone biopsy) [11,12], in which TGFβ1 acts as a chemoattractant, recruiting osteoprogenitor/stem cells and stimulating osteogenic differentiation and matrix production at bone formation sites. During OA subchondral bone remodeling, elevated local TGFβ1 concentrations exacerbate subchondral bone loss in early stage and lead to sclerosis during OA progression mainly by inducing the vascularization and hypomineralization of osteoblasts [13]. The TGFβ1 concentration is significantly higher in OA joints than in healthy joints: the average TGFβ1 concentration is less than 1 ng/mL in the synovial fluid of healthy joints, but it reaches to 2–5 ng/mL in the synovial fluid of OA knee joints [11]. Overactivated TGFβ signaling, which causes synovitis, cartilage degradation, and subchondral bone pathogenesis, was detected in OA knee specimens collected from both human and mice. Recently, Muratovic et al. demonstrated that human OA subchondral bone underneath damaged cartilage had a significantly higher concentration (>26.4 pg/mL) of active TGFβ1 than paired relatively normal subchondral bone underneath intact cartilage (4.3 pg/mL), and that an increased concentration of active subchondral TGFβ1 was spatially associated with impaired bone quality and disease severity [10]. Thus, inhibiting excessive TGFβ1 in early OA joints can be a potential therapeutic target to prevent OA progression in subchondral bone.

Several pre-clinical studies reported positive effects of blocking elevated TGFβ1 signaling in OA animals by using small molecules (*e.g.,* SB-505124, halofuginone, and artesunate) [14–17] or a neutralizing antibody (1D11) [18], or knocking out TGFβ receptor II in chondrocytes [19]. However, due to the fundamental role of TGFβ signaling in cell survival and function, systemic inhibition of TGFβ can also lead to serious side effects such as cardiovascular toxicity, oncogenesis and gastrointestinal symptoms [20], local inhibition of excessive TGFβ and its activity in OA joints has a higher safety level from the perspective of clinical application.

Pirfenidone (PFD) is a pyridine [5-methyl-1-phenyl-2-(1H)] small-molecule inhibitor of TGFβ1-3. It exerts anti-fibrotic and anti-inflammatory effects by targeting the TGFβ signaling pathway and has been clinically applied to treat pathological fibrosis, including idiopathic pulmonary fibrosis, liver fibrosis and renal fibrosis [21,22]. As a broad-spectrum anti-fibrotic drug, PFD also reduce other inflammatory mediators such as tumour necrosis factor alpha (TNFα) and interleukin (IL)-1β, thus exerting anti-inflammatory effects [23,24]. The application of PFD in injured or diseased joints was recently investigated. Studies in rats with collagen-induced arthritis have shown that PFD treatment is associated with down regulation of matrix metalloproteinase-3 (MMP-3) and vascular endothelial growth factor in chondrocytes and synovial cells [23]. In OA, Chan et al. reported that oral PFD treatment reduced subchondral bone loss and joint-wide fibrosis in a murine knee cartilage injury model [25]. Wei et al. reported that the daily oral administration of PFD (30 mg/kg body weight daily, 4 weeks) attenuated synovial fibrosis and OA development in rabbits with anterior cruciate ligament transection induced OA [26]. These studies have provided pre-clinical evidence of the effectiveness of oral PFD treatment in relieving synovium inflammation, regulating subchondral bone and maintaining cartilage health. Notably, the above studies used PFD orally. In the case of treating patients with idiopathic pulmonary fibrosis, the recommended oral application dosage of PFD for maintaining a stable and effective concentration in the plasma is 801 mg per serve, three times daily (*i.e.,* 2403 mg per day) for more than 1 year [27]. The long-term, high doses of oral PFD could lead to a wide range of side effects, including nausea, photosensitivity and gastrointestinal issues [27,28]. Therefore, here we report a new and effective strategy to locally target excessive TGFβ in early OA joint *via* the controlled-release of the clinically approved TGFβ inhibitor, PFD, as a safer and effective potential OA treatment.

Aiming to maintain an effective dose of PFD and achieve local inhibition of excessive TGFβ and its activity in OA-affected joints, we adopted poly (lactic-*co*-glycolic acid) (PLGA), a Food and Drug Administration (FDA)-approved polymeric carrier [29] to encapsulate and control the local concentration of PFD by generating PFD-loaded PLGA microspheres (PFD-PLGA-MS). PLGA has excellent biocompatibility and biodegradability, and is widely used to sustainably release small molecules, and as a molecular drug carrier, the small molecules encapsulated in PLGA can be released in a controlled and gradual manner by controlling the size, shape, and degradation rate of the biomaterial [29,30]. Meanwhile, in terms of maintaining an effective dosage of PFD for longer periods of time in OA joint, the active synovial lymphatic drainage function is another consideration [31]. The free PFD released from PLGA can be rapidly removed from joint cavity without a suitable macromolecular carrier. Therefore, in this study, we also incorporated a clinically used HA solution as an integral drug carrier of PFD-PLGA-MS to enhance the retention of both PFD-PLGA-MS and free PFD in the affected joints. With the incorporation of biomaterials, we simplified the treatment to monthly I.A. injections (the "PFD–PLGA + HA" strategy), and after three injections, we observed a joint-wide therapeutic effects including subchondral bone remodeling, synovitis and pain reduction, and cartilage preservation in the treatment groups. These encouraging results support the great potential of this strategy as a novel and convenient DMOAD treatment of OA, particularly at the early stage.

3. Results

3.1. Uncoupled bone remodeling in early OA subchondral bone

To observe sequential subchondral bone changes in OA mice, the microstructure of proximal medial tibia subchondral bone was evaluated by micro-computed tomography (μCT) on days of 3, 7, 10, 14, 21, 28 56, 84, and 112 after destabilization of the medial meniscus (DMM)

surgery (Fig. 1A–D). The joint subchondral bone displayed an osteoporotic phenotype from 7 days to 28 days after DMM (yellow arrows in Fig. 1A). The decrease in bone mineral density (BMD, mgHA/cm^3) and bone volume fraction (BV/TV, %) initiated as early as 7 days after DMM (Fig. 1C, BMD, DMM side: 548.589 ± 17.164 mgHA/cm^3 *vs.* contralateral side: 473.431 ± 18.093 mgHA/cm^3, *p=0.003*; Fig. 1D, BV/TV, DMM side: 46.552 ± 2.308 % *vs.* contralateral side: 39.154 ± 2.433 %, *p=0.029*), and the bone loss was further aggravated at day 28 in comparison with contralateral knee joint (Fig. 1C, BMD, DMM side: 509.927 ± 17.164 mgHA/cm^3 *vs.* contralateral side: 601.337 ± 18.093 mgHA/cm^3, $p < 0.001$; Fig. 1D, BV/TV, DMM side: 42.417 ± 2.308 % *vs.* contralateral side: 54.412 ±0 .433 %, $p < 0.001$).

As OA progressed, OARSI score increased (Fig. S1), and the subchondral bone underwent sclerosis and the bone volume increased significantly after 56 days. Bone mineral density and bone volume elevated at 56, 84 and 112 days after DMM, and reached the highest level at 112 days (Fig. 1C, BMD, day 112: 710.030 ± 86.434 mgHA/cm^3; Fig. 1D, BV/TV, day 112: 65.433 ± 10.509 %). The corresponding cell types of Trap$^+$ osteoclasts, subchondral Cathepsin K$^+$ osteoclasts, Osterix$^+$ osteoprogenitors, and Ocn$^+$ mature osteoblasts were also increased, demonstrated by histological staining and quantification of the cells in OA subchondral bone (Fig. S2).

3.2. PFD alleviate the excessive TGFβ1 incurred hypomineralization in vitro

We then evaluated the potential subchondral bone-regulating effects of PFD (Fig. 1E) at concentrations of 0, 30, 100 and 500 μg/mL (without affecting cell viability, Fig. S5) on the osteoblast cell line Saos-2 and primary human bone marrow-derived stem cells (hBMSCs, from three biological donors, characterized in Fig. S4) exposed to high concentrations of TGFβ1 in the culture medium (Fig. 1F–H, Fig. S3). We found that PFD at 100 μg/mL attenuated excessive TGFβ1-induced hypomineralization in Saos-2 cells and primary hBMSCs at the local TGFβ1 concentrations (2 and 5 ng/mL) observed in OA subchondral bone (Fig. 1F–H).

Specifically, in the growth medium, the supplementation of TGFβ1 (2 and 5 ng/ml) nor PFD (30, 100, and 500 μg/ml) had strong effects on the mineralization of Saos-2 cells (Fig. 1G, group A-F), suggesting that PFD did not affect the normal mineralization of osteoblastic cells. OM induction effectively enhanced Saos-2 cells mineralization at a high level (Fig. 1F; Fig. 1G, Group G). Meanwhile, supplementation of TGFβ1 (2 and 5 ng/mL) significantly impaired the Von Kossa staining intensity (Fig. 1G; Group K - TGFβ1, 2 ng/ml: 20.08 ± 3.73 % *vs.* Group G - OM: 31.17 ± 7.82 %, *p=0.003*; Group O - TGFβ1, 5 ng/ml: 17.9 ± 2.02 % *vs.* Group G - OM: 31.17 ± 7.82 %, *p=0.008,* full comparison results in Table S4). Without TGFβ1 in OM, treatment of PFD at 30, 100, and 500 μg/ml did not change the mineralization significantly (Fig. 1G, Group H-J). In the TGFβ1-treated groups (2 or 5 ng/mL in OM), PFD significantly restored the TGFβ1-incurred impaired mineralized property of Saos-2 cells at the level of 100 μg/ml (Fig. 1G, Group M − PFD + TGFβ1, 2 ng/mL: 25.10 ± 4.36 %, *vs.* Group K - TGFβ1, 2 ng/mL: 20.08 ± 3.73 %; *p=0.047;* Group Q - PFD + TGFβ1, 5 ng/mL: 23.45 ± 2.37 % *vs.* Group O - TGFβ1, 5 ng/mL: 17.90 ± 2.02 %, *p=0.045*). Similar effects were found in hBMSCs *i.e.,* TGFβ1 at both 2 and 5 ng/mL reduced the mineralization density of hBMSCs by 63 % and 69 %, respectively (Fig. 1F, **H**: 21 days; Fig. S3). PFD supplementation at 100 μg/mL in OM for 21 days significantly ameliorated TGFβ1-inccurred hypomineralization (Fig. 1F–H; PFD + 5 ng/mL TGFβ1: 49.03 ± 4.42 % *v.s* 5 ng/mL TGFβ1: 18.65 ± 2.90 %, *p=0.018*).

The above *in vitro* data provided supporting evidence for the potential application of PFD for regulating OA subchondral bone. We next aimed to deliver and maintain PFD at the determined effective dosage (*i.e.*, 100 μg/ml, Fig. 1F–H) in early OA knee joints.

3.3. Design, fabrication of PFD-PLGA-MS for sustained release PFD

To achieve sustained release of PFD *in vivo*, the biodegradable biomaterial PLGA was used to encapsulate PFD and PFD-loaded PLGA-MS (PFD–PLGA-MS) were generated following the principles of biofabrication (Fig. 2A).

The structure of the microspheres was characterized using a stereomicroscope under bright field and scanning electron microscopy (SEM) after lyophilization. Both blank PLGA (PLGA-MS) and PFD-PLGA-MS displayed spherical shape with smooth surfaces (Fig. 2B), and a narrow particle size distribution (Fig. 2B and C). The average radius of the PFD-PLGA-MS was 1322.63 ± 266.93 nm, which was consistent with the result of SEM imaging (Fig. 2C).

The drug loading efficacy was estimated by measuring the absorbance at 311 nm wavelength after dissolving pirfenidone loaded nanoparticles in DCM followed by extraction into water. The loading efficacy of PFD in PLGA microparticle is 19.21 % ± 3.54 (192.1 ± 35.4 μg/mg particle). The encapsulation efficiency was 91.13 % ± 7.45. The drug release property of PFD–PLGA-MS was evaluated using a cumulative release curve (Fig. 2D, E; 5 mg of microparticles in 1 mL of phosphate-buffered saline [PBS]). The PFD release kinetics were assessed using an ultraviolet spectrophotometer (absorbance at 330 nm wavelength). The PFD-PLGA MS showed a burst release of nearly 28.3 % total PFD within the first day, and started gradually plateauing thereafter (Fig. 2D), and the remaining PFD was slowly released over 28 days and the PFD concentration in the medium was maintained at 112.08 μg/mL (Fig. 2E).

The pH of the supernatant of the PFD–PLGA-MS controlled release system was further evaluated to address the potential risk of acid-induced cartilage damage due to the biodegradation of PLGA polymers (lactic and glycolic acids). PFD-PLGA-MS showed a similar pH pattern to the blank PLGA-MS and it was around 7 at all timepoints, suggesting a stable and safe acid-base environment (Fig. 2F). Considering that the pH in OA knee is 7.3 (ranging from 6.8 to 7.68) [32], we then used PBS solution with different pH values (6.8 and 7.4) to mimic the acidic microenvironment of osteoarthritic joint and normal healthy joint. We measured the release characteristics of PFD-PLGA MS within the pH 6.8 and pH 7.4 at 1, 3, 7, 14, and 28 days after MS dissolution. The long-term cumulative release curve was shown in Fig. S6. Generally, compared with normal pH PBS (pH: 7.4), the acid microenvironment (pH: 6.8) accelerated the MS degradation rate and induced more PFD release at each time points, though without significant difference ($p > 0.05$).

We further dissolved the PFD-PLGA-MS into HA solution (5 mg of microparticles in 1 mL of 1.5 % HA) and compared its release curve with PFD-PLGA-MS in PBS (5 mg of microparticles in 1 mL of PBS). The release curve of PFD in HA showed a similar burst release of nearly 30 % (33.9 ± 5.5 %, Fig. 2G) PFD within the first 3 days, and a significantly better PFD retention at 21, 28, and 35 days of dissolving than PBS (Fig. 2G).

To elucidate the *in vivo* clearance of PFD-PLGA MS, we employed a small molecule fluorescent indocyanine green (ICG) to trace the particle degradation and clearance in OA joint as previously described [33]. After 7 days of DMM surgery, mice were I.A. injected with ICG-PLGA + HA MS and ICG in PBS solution. The retention of MS was assessed through fluorescence imaging with an *in vivo* imaging system (IVIS) at days 0, 1, 3, 7, 14, 21, and 28 respectively. From IVIS results, joints that received ICG-PLGA HA injection displayed intensified fluorescence signals, and longer retention duration compared to those injected with ICG only over the investigated period (Fig. 2H and I). Semiquantitative analysis of the AUC (area under the curve) based on the fluorescence intensity profiles indicated that retention of ICG-PLGA + HA in joints with OA condition was greater than that of ICG only joints (ICG only *vs.* ICG-PLGA + HA: 1.45 x 10^9 ± 5.9 x 10^8 *vs.* 3.2 x 10^9 ± 1.0 x 10^9, $p = 0.0023$, Fig. 2J). These results confirmed the prolonged retention effects of PLGA MS HA solution.

Thus, we established a practical way to prolong the sustained release

of PFD at the functional concentration for up to 4 weeks both *in vitro* and *in vivo*.

3.4. The "PFD–PLGA + HA" strategy for early OA treatment

Based on above results, we advanced the PFD delivery strategy into a monthly I.A. injection therapy in which PFD–PLGA-MS was injected in combination with HA into OA knee joints every 4 weeks (Fig. 3A, the "PFD–PLGA + HA strategy", *patents filed*). The involvement of HA here is in consideration of the drug and water retention effect of HA as a macromolecule to achieve local delivery of PFD in the joint cavity; we have also examined the release curve of PFD-PLGA-MS in HA and the PFD retention was significantly higher in HA compared to the PBS group (Fig. 2E, HA *vs.* PBS, Day 21: $p=0.025$; Day 28: $p=0.016$; Day 35: $p=0.0154$). This therapeutic strategy was then validated in mice with DMM-induced OA in comparison with the commercial HA Ostenil® as one of the control groups. The detailed animal study design is provided in Table S1 and Fig. 3A; the animals received monthly I.A. injections of

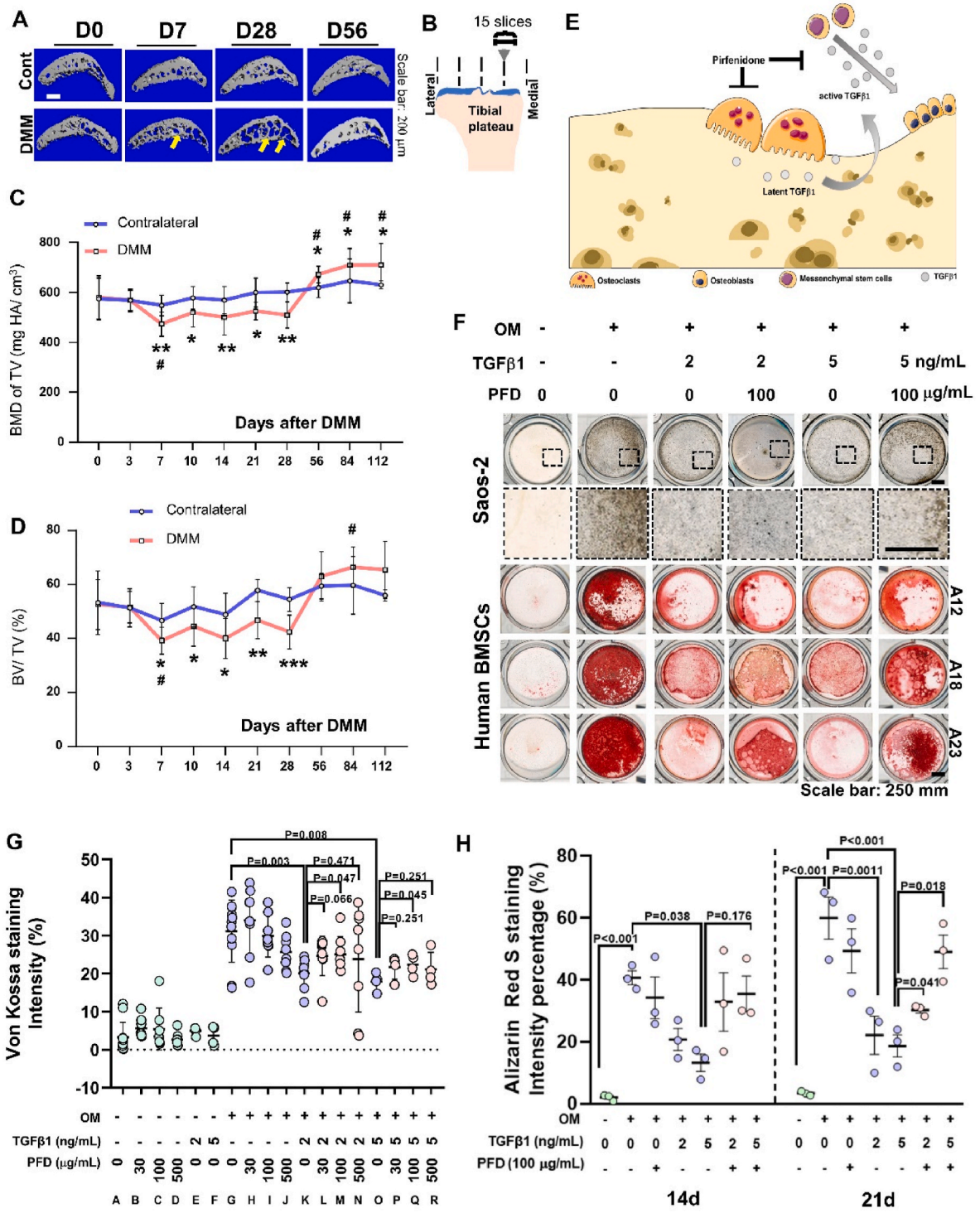

(caption on next page)

Fig. 1. Targeting early OA by regulating subchondral bone changes: PFD attenuated cell hypomineralization caused by the overexpression of TGFβ1.
(A) Time-dependent phenotypic alterations of OA subchondral bone in mice with DMM-induced OA at days of 0, 7, 10, 14, 21, 28, 56, 84 and 112. Representative sagittal photographs of knee joint sections at days 0, 7, 28, and 56. Upper: non-operated knee; bottom: DMM-induced OA knee. **(B)** Schematic diagram for selecting regions of interest for μ-CT quantification. **(C)** Quantification of BMD of DMM-induced OA joints; n = 8 in each group. Data are mean ± SD; *$p < 0.05$, **$p < 0.01$ *vs.* parameters in contralateral sides in corresponding timepoints; #p < 0.05 *vs.* the parameters in the baseline (Day0). **(D)** Quantification of BV/TV% of DMM-induced OA joints, n = 8 in each group, data are mean ± SD; *$p < 0.05$, **$p < 0.01$, ***$p < 0.001$ *vs.* parameters in contralateral sides in corresponding timepoints; #P < 0.05 versus the parameters in the baseline (Day0). **(E)** Schematic diagram for the hypothesis of targeting bone remodeling in OA subchondral bone: over-release of active TGFβ1 during bone remodeling contributes to hypomineralization and osteosclerosis, and a TGFβ inhibitor pirfenidone (PFD) could effectively restore the mineralization in osteoblastic cells such as osteoblasts and MSCs. Additionally, PFD can also inhibit the osteoclastogenesis and maturation to maintain the balance of bone remodeling. **(F)** PFD attenuated the excessive TGFβ1-incurred hypomineralization in bone forming cells. Representative images of Von Kossa staining from Saos-2 cells (upper panel, 24 well plate, bar = 250 μm) and Alizarin Red S staining from hBMSCs (lower panel, 3 biological donors, cells were cultured in 24 well plate, bar = 250 μm) treated with PFD (100 μg/ml) and/or TGFβ1 (2 or 5 ng/ml) in growth medium (GM) and osteogenic medium (OM). **(G)** PFD attenuated excessive TGFβ1-incurred hypomineralization in Saos-2 cells in dosage dependent manner. Quantitative results of Von Kossa staining from Saos-2 cells treated with PFD (0, 30, 100, 500 μg/ml) and/or TGFβ1 (2 or 5 ng/ml) in GM or OM for 14 days. The experiment was performed at least twice with at least triplicates as technical repeats; Data are mean ± SD values from readouts quantified from each well, n = 4–8; One-way ANOVA, followed by Bonferroni test was used to evaluate the statistical difference. All *p* values are as labeled, and detailed p values between groups are in Table S2. **(H)** PFD attenuated TGFβ1-incurred hypomineralization in hBMSCs. Quantitative results of Alizarin Red S staining from primary isolated hBMSCs treated with PFD (100 μg/ml) and/or TGFβ1 (2 or 5 ng/ml) in GM or OM for 14 days and 21 days. Data are mean ± SD values collected from 3 individual biological donors (n = 3 biological donor in the dot plot, donor code No. A12, A18 and A23), and each assay was performed with at least triplicates as technical repeats. One-way ANOVA, followed by Bonferroni test was used to evaluate the statistical difference. p values are as labeled, and the characterization of hBMSCs and images of the Alizarin Red S staining at day 14 are shown in Figs. S3 and S4.

PFD–PLGA-MS at various timepoints after DMM (*i.e.,* at 1, 5 and 9 weeks after DMM) during a 12-week follow-up period. The subchondral bone changes, pain-related behaviour, OA progression-related histological scores and possible therapeutic mechanisms were assessed.

3.5. Monthly injection of PFD–PLGA + HA regulates OA subchondral bone remodeling

At the beginning of OA, an osteoporotic phenotype in subchondral bone area was found in the animals at first 4 weeks after DMM (Fig. 1A–D). To observe whether the sustained release of PFD had a subchondral bone-remodeling effect of in early OA joints, we first investigated the structural changes in subchondral trabeculae (Trab) in the load-bearing area with μCT (Fig. 3B–E). We found a significantly higher BMD and BV/TV in the subchondral Trab in the PFD–PLGA + HA group than in the commercial HA control group during early OA development (Fig. 3C–E, 2 and 4 weeks after DMM). The PFD–PLGA + HA group had the lowest bone loss in Trab among seven groups; in particular, bone loss after PFD–PLGA + HA treatment was significantly lower than that after commercial HA treatment at 2 weeks after DMM (Fig. 3D, BMD: PFD–PLGA + HA: 533.823 ± 19.555 *vs.* commercial HA: 504.310 ± 26.375, $p=0.039$; Fig. 3E BV/TV: PFD–PLGA + HA: 48.808 ± 2.383 *vs.* commercial HA: 41.918 ± 3.807, $p=0.098$) and 4 weeks after DMM (Fig. 3D, BMD: PFD–PLGA + HA: 627.375 ± 27.092 *vs.* commercial HA: 446.865 ± 40.709, $p=0.015$; Fig. 3E, BV/TV: PFD–PLGA + HA: 57.852 ± 2.733 *vs.* commercial HA: 42.708 ± 6.094, $p=0.032$).

After OA progression, only total subchondral bone was analyzed (Fig. 3F and G) at 8 and 12 weeks after DMM because the subchondral bone plate and Trab fused and became sclerotic (Fig. 1A, day 56–84). Compared with healthy joints (Fig. 3 F, G; dashed lines), the PBS group showed a high bone volume and mineral density at 8 and 12 weeks after DMM, indicating a sclerotic tendency in animals without treatment. Notably, PFD–PLGA + HA treatment attenuated the aberrantly elevated subchondral bone volume at 12 weeks after DMM (Fig. 3F, BMD: PFD–PLGA + HA: 619.064 ± 23.116 *vs.* PBS: 674.176 ± 24.575, $p=0.029$).

The above data indicate that the PFD–PLGA + HA therapy has a subchondral bone remodeling effect in early OA mice, and monthly I.A. injections of PFD–PLGA + HA help maintain a healthy subchondral BMD and structure for up to 12 weeks after DMM surgery.

3.6. PFD–PLGA + HA treatment regulates OA subchondral bone by reducing the activation of TGFβ signaling via Smad2/3

In vitro experiments revealed that PFD had a hypomineralization-rescuing effect in osteoblasts and hBMSCs under the stress of excessive TGFβ present in culture environment (Fig. 1E–H). To observe the *in vivo* effect of PFD on subchondral bone in OA knee joints, we evaluate the activation levels of TGFβ1 signaling by examining the protein expression level of phosphorylated Smad2/3 (pSmad2/3) in the subchondral bone areas of mice with DMM-induced OA in all of the seven treatment groups (Fig. 3H and I).

Compared with healthy knee joints, pSmad2/3 was upregulated in osteoarthritic subchondral bone at 4 and 12 weeks after DMM (Fig. 3H and I; PBS group). The ratio of pSmad2/3-positive cells in subchondral bone zone was significantly higher in both early and late stages of OA (Fig. 3I , 4 weeks post-DMM-PBS: 533.08 ± 108.08 cells/mm^2 *vs.* age-matched healthy knee: 134.73 ± 44.95 cells/mm^2, $p < 0.001$; 12 weeks post-DMM-PBS: 461.85 ± 72.57 cells/mm^2 *vs.* age-matched healthy knee: 127.97 ± 19.73 cells/mm^2, $p < 0.001$). Like PBS group, I.A. administration of commercial HA showed similarly high level of pSmad2/3 at both 4 and 12 weeks after DMM to those of healthy knees (Fig. 3H and I), suggesting that the increased activation of TGFβ signaling in OA subchondral bone was not rescued by commercial HA treatment. Remarkably, the monthly I.A. injection of PFD–PLGA + HA treatment maintained a low activation level of TGFβ signaling in OA subchondral bone (Fig. 3H and I). Fewer pSmad2/3$^+$ cells were found in PFD–PLGA + HA group compared to PBS group at 4 weeks after DMM (Fig. 3H and I; 4 weeks: PFD–PLGA + HA group, 336.80 ± 57.99 cells/mm^2 *vs.* PBS, 533.08 ± 108.08 cells/mm^2, $p=0.0234$), and less pSmad2/3$^+$ cells were found in PFD–PLGA + HA group compared to commercial HA group at 12 weeks after DMM (Fig. 3H and I; 12 weeks: PFD–PLGA + HA group, 313.66 ± 38.96 cells/mm^2 *vs.* Commercial HA, 504.79 ± 110.06 cells/mm^2, $p=0.0295$), suggesting that the effect of PFD on subchondral bone remodeling in OA joints occurs through the modulation of overactivated TGFβ signaling.

3.7. Monthly I.A. Injection of PFD–PLGA + HA ameliorated OA progression in DMM-induce OA mice

OA progression was then assessed histologically in DMM-induced OA joints, and graded by cartilage morphology, osteophyte formation and total OARSI score (Fig. 4). In the PBS group, proteoglycan loss in the cartilage surface started at 2 weeks after DMM, which was further aggravated at 4 weeks after DMM and progressed into a severe cartilage cleft and erosion at 12 weeks after DMM (Fig. 4A, black boxes). In the commercial HA treatment group, articular cartilage was retained in normal shape at both 2 and 4 weeks after DMM, indicating a protective effect of commercial HA against articular cartilage degeneration during early-stage OA (Fig. 4A, black boxes). However, severe cartilage erosion and fibrillations were found at 12 weeks after DMM in commercial HA

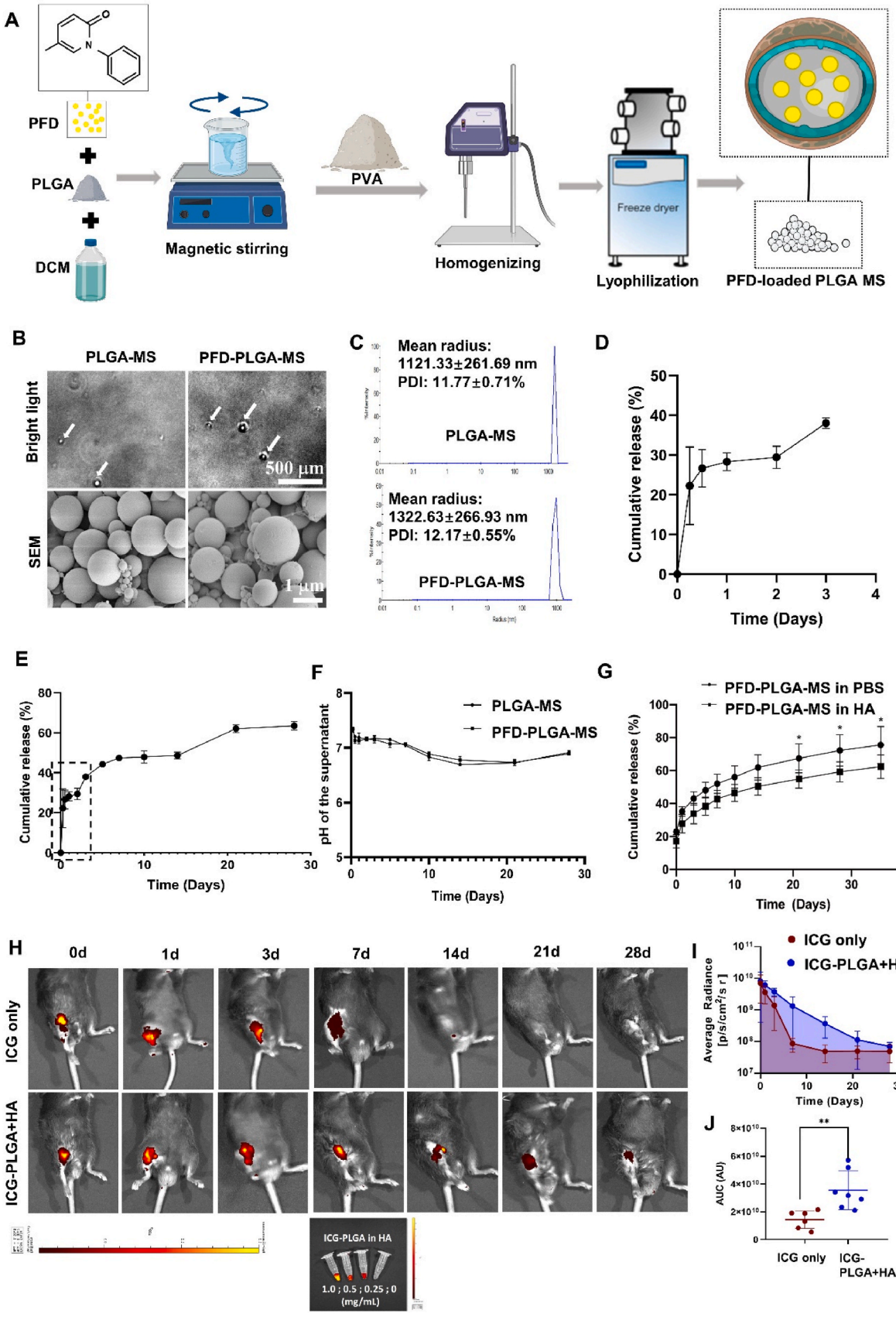

(caption on next page)

Fig. 2. Preparation and characterization of the PFD-loaded PLGA microsphere (PFD-PLGA MS)
(A) Workflow of PFD-PLGA-MS fabrication. PFD: Pirfenidone; PLGA: Poly lactic-*co*-glycolic acid; PVA: Polyvinyl alcohol. **(B)** Representative images of PLGA-MS (blank control) and PFD-PLGA-MS under a stereotype microscope (upper, bar = 500 μm) and SEM (lower, bar = 1 μm). **(C)** Dynamic lightning scatter measurement of particle size; n = 3. (**D** and **E**) Cumulative short-term burst release curve of PFD-PLGA-MS (5 mg particles in 1 mL PBS, total medium changed daily) in PBS from day 0 to day 4, and **(E)** cumulative long-term release curve of PFD-PLGA-MS in PBS for up to 28 days, evaluated by the absorbance at 330 nm wavelength. Each experiment was performed independently with 3 technical repeats, and results are present by means ± SD. **(F)** pH of the supernatant in the release curve. **(G)** Cumulative long-term release curve of PFD-PLGA-MS in PBS and HA solution (1.5 %) for up to 35 days. Each experiment was performed independently with 3 technical repeats, and results are presented as means ± SD. **(H)** Joint retention of ICG-labeled PLGA + HA solution. Representative fluorescence images of knee joints from OA mice over 0, 1, 3, 7, 14, 21, and 28 days after intra-articular injection of free ICG (ICG), and ICG-labeled PLGA MS + HA (ICG-PLGA + HA) respectively. The *in vitro* fluorescence image of ICG-PLGA + HA solution (with different concentrations of 1.0, 0.5, 0.25 and 0 mg/ml) was shown in the lower panel. **(I)** Quantitative analysis of the time course of relative fluorescence radiant efficiency within knee joints after intra-articular injection. n = 6–7/group. **(J)** Semiquantitative analysis of the AUC based on the average radiance (n = 6–7). AUC, area under the curve. AU, arbitrary units. Statistical analysis was performed using the Mann-Whitney *U* test. The data were presented as means ± SD, with ** $p < 0.01$ indicating statistical significance.

treated group, with nearly all hyaline cartilages worn out (Fig. 4A, black boxes), suggesting a short-term cartilage protection effect of commercial HA. Notably, in the PFD–PLGA + HA group, intact cartilage was found at early OA joints (Fig. 4A, 2 and 4 weeks after DMM), and retained cartilage surface, although some degree of cartilage proteoglycan loss and fibrillation was found at 12 weeks after DMM (Fig. 4A, black boxes). The OARSI score revealed that our treatment strategy had a long-term regulative effect in OA progression: the PFD–PLGA + HA group showed significant lower OARSI scores than the PBS group and commercial HA group at 12 weeks after DMM (Figs. 4B, 12w: PFD–PLGA + HA: 3.00 ± 0.94 *vs.* PBS: 5.00 ± 0.50, $p=0.0026$; PFD–PLGA + HA: 3.00 ± 0.94 *vs.* commercial HA: 5.00 ± 1.15, $p=0.0093$).

Osteophyte formation is another pathological phenotype of OA. Less osteophyte formation was found at all evaluated timepoints in PFD-PLGA + HA group than in the PBS group (Fig. 4A, dash box), with a significantly reduced osteophyte maturity score (Fig. 4C; 2 weeks, PFD–PLGA + HA: 0.500 ± 0.204 *vs.* PBS: 1. 667 ± 0.192, $p=0.046$; 4 weeks, PFD–PLGA + HA: 0.833 ± 0.152 *vs.* PBS: 2.000 ± 0.152, $p=0.026$; 12 weeks, PFD–PLGA + HA: 1.667 ± 0.304 *vs.* PBS: 2.833 ± 0.152, $p=0.039$). As another control group, the commercial HA group showed similarly poor effects to the PBS control group in terms of preventing osteophyte formation at all of the evaluated timepoints (Fig. 4C; 2 weeks, commercial HA: 1.167 ± 0.152 *vs.* PBS: 1.667 ± 0.192, $p=0.973$; 4 weeks, commercial HA: 1.833 ± 0.281 *vs.* PBS: 2.000 ± 0.152, $p=0.837$; 12 weeks, commercial HA: 2.667 ± 0.471 *vs.* PBS: 2.833 ± 0.152, $p > 0.990$). The PFD–PLGA + HA group showed a lower osteophyte score than the commercial HA group at 12 weeks after DMM (Fig. 4C; 12 weeks: PFD–PLGA + HA: 1.167 ± 0.89 *vs.* commercial HA: 2.667 ± 0.471, $p=0.014$), suggesting a better disease-modify effect compared to current HA treatment.

3.8. Monthly injection of PFD–PLGA + HA attenuated pain-related behaviors in OA animals

To observe whether the monthly I.A. injections of PFD–PLGA + HA provided symptom relief, we tracked the gait parameters, including the pawprint area, intensity, step length, duration and walking speed, of mice with DMM-induced OA for up to 12 weeks (Fig. 5A). Briefly, mice were subjected to monthly I.A. injections with different components (Fig. 3A–Table S1) from 1 week after DMM, and the treatments were applied at 1, 5 and 9 weeks after DMM. Animal gait parameters were measured before (Fig. 5B) and after DMM surgery, at 1 week after DMM, and then were longitudinally tracked at 2, 3, 4, 6, 8, and 12 weeks after DMM (Fig. 5C). Healthy joints give a large pawprint area, while a reduced pawprint area indicates less contact with the ground and reduced willingness to load, mainly due to joint pain and dysfunction [34]. The mice in the PFD–PLGA + HA group demonstrated the largest pawprints of the right hindlimb (DMM-induced OA side) at all timepoints (Figs. 5C, 4 and 6, 8, 12 weeks after DMM), and the heatmap of the pawprint also indicated that the hindlimb force was highest in the DMM-induced OA knee (Fig. 5C).

Next, we evaluated the load-bearing properties of DMM-induced OA joints based on the maximal contact intensity of pawprints and found that monthly injections of PFD–PLGA + HA attenuated the DMM induced force impairment in lower limbs (Fig. 5B–D). The PBS group showed a negative intensity (Δ value < 0, compared with 1 week after DMM) at all subsequent timepoints, indicating that I.A. administration of PBS in DMM mice did not reverse the pain compared to the pre-treatment status. In PLGA-HA and HA treatment groups, the joint load-bearing property was similarly affected (Fig. 5D, Δ value < 0, PBS group: blue; PLGA-HA group: green; HA group: purple). In contrast, the PFD–PLGA + HA group showed improvement in maximal contact intensity compared to pre-I.A injection in almost all timepoints (Fig. 5D, PFD–PLGA + HA group: orange; 2, 3, 8, 12 weeks after DMM, Δ value > 0). Specifically, among all treatments, only PFD–PLGA + HA group showed significant higher maximal contact intensity value compared to PBS group at both 4 and 8 weeks after DMM (Fig. 5D; 4w, PFD–PLGA + HA: 2.484 *vs.* PBS: −3.763, $p=0.0161$; 8w: PFD–PLGA + HA: 2.178 *vs.* PBS: −4.353, $p=0.0006$), suggested an effective long-term pain relief effect of PFD–PLGA + HA treatment. In addition, the PFD + HA treatment group showed higher pawprint intensity at the very early stage of OA development (Fig. 5D, PFD + HA, red; Δ value > 0 at 2 and 4 weeks after DMM) compared to pre I.A. injection. But the protective effect of PFD + HA did not last long (Fig. 5D, PFD + HA, red; 8 and 10 weeks after DMM, Δ value < 0), indicating temporary pain relief effects of PFD, and a crucial role of sustained release of PFD locally at an effective dose.

We also evaluated spatial parameters by analyzing Δprint area (Fig. 5E), in which the positive value represents the increased pawprint area of DMM-induced OA hind and contralateral hind (RH/LH) compared to the pre-I.A. injection (1 week after DMM surgery). Compared to the pre-I.A. injection, I.A injection of PBS displayed the less pawprint area at all timepoints (Fig. 5E, PBS group in blue, Δvalue<0 at all timepoints), which build a baseline of untreated OA joints. Among all treated groups, only PFD–PLGA + HA group showed increased print area at all timepoints (Fig. 5E, PFD–PLGA + HA, orange, Δvalue>0 at all timepoints), suggesting the best recovered joint loading condition in PFD–PLGA + HA treatment group in the DMM-induced OA joints. At 4 and 12 weeks post-DMM, the PFD–PLGA + HA group showed significantly larger print area in comparison with PBS group (Fig. 5E, Δ Print area%: 4w: PFD–PLGA + HA: 8.85 *vs.* PBS: −17.36, $p=0.005$; 12w: PFD–PLGA + HA: −13.47 *vs.* PBS: 18.61, $p=0.011$). These results indicated that I.A. injection of PFD–PLGA + HA efficaciously alleviated OA-incurred pain-related behavior in mice. Other parameters of gait analysis, the duty cycle (Fig. 5F) and limb idleness index (Fig. 5G) demonstrated similar trends – as a control, PBS treatment caused less duty cycle in DMM mice and higher limb idleness index, and PFD–PLGA + HA group increased the duty cycle and reduced limb idleness index significantly (Fig. 5F and G).

Altogether, the above results indicate that monthly I.A. administration of PFD–PLGA + HA attenuated pain-related behaviors in mice with DMM-induced OA for up to 12 weeks.

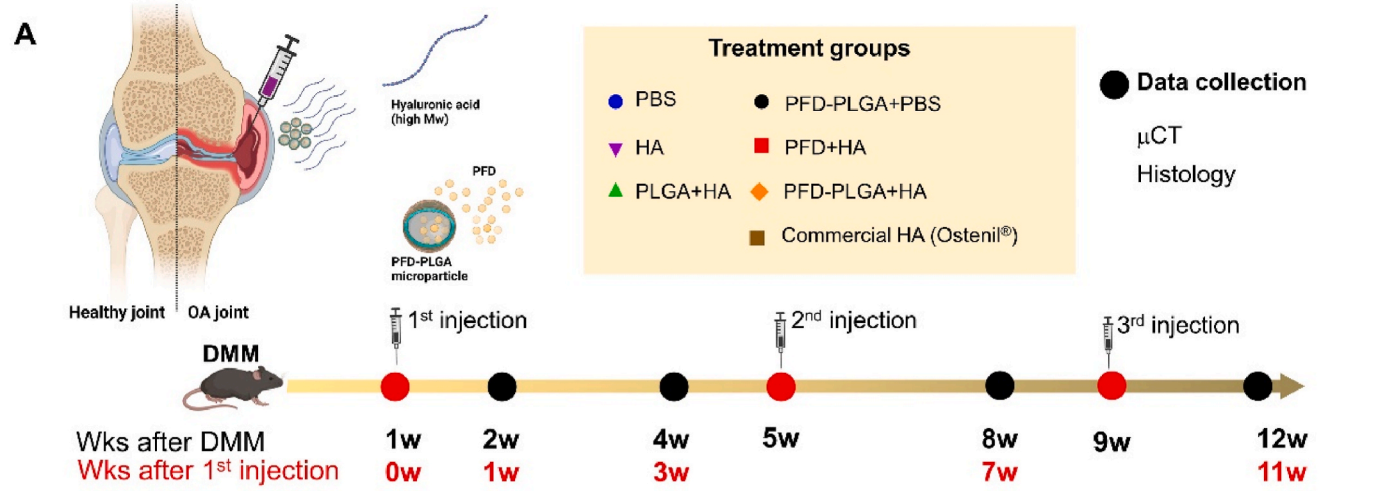

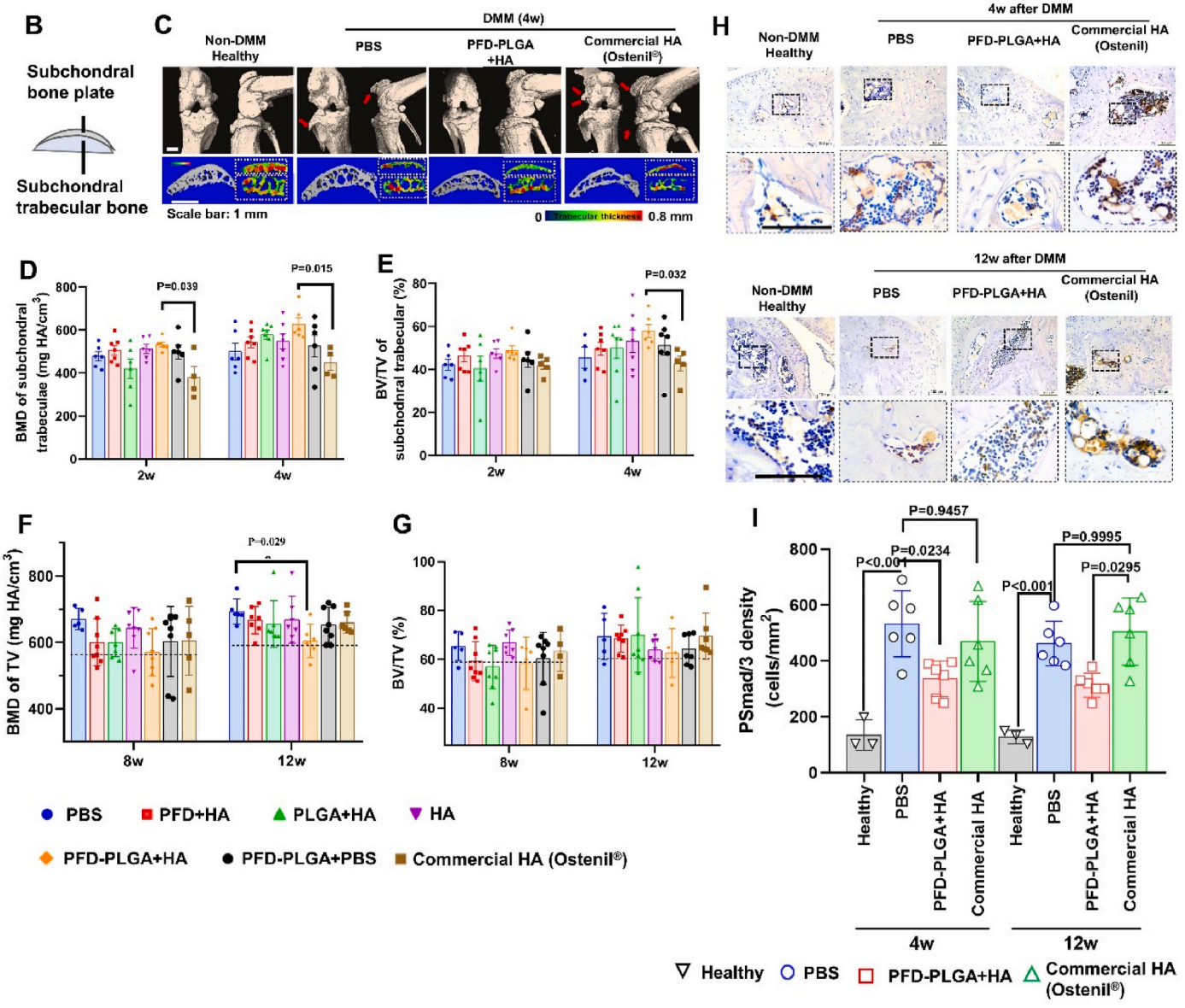

(caption on next page)

Fig. 3. Monthly I.A. injection of PFD–PLGA + HA attenuated subchondral bone structural changes in OA mice joints
(A) Illustration of the "**PFD–PLGA + HA**" treatment strategy and *in vivo* study design. DMM surgery was performed on murine right knee joints, and monthly I.A. administration of different treatments was performed at 1, 5 and 9 weeks after DMM. Details about the groups are in Table S1. **(B)** ROIs of mice subchondral bone for data analysis: the subchondral bone plate and subchondral trabecular bone (Trab). **(C)** Representative 3D reconstructive μCT results of knee joints, obtained from PBS, PFD–PLGA + HA and commercial HA treatment groups after 4 weeks of DMM, with healthy joints as controls for comparison. Upper panel, 3D reconstructive μCT results of knee joints from the sagittal and frontal views; red arrows, osteophytes. Lower panel, representative 3D color map images showing detailed bone thickness within tibial subchondral bone plate and subchondral trabeculae. Color ranges from 0 mm (green) to 0.8 mm (red); scale bar = 1 mm. **(D)** Quantification of bone mineral density and **(E)** bone volume of subchondral trabeculae at early OA stages (Trab, 2 weeks and 4 weeks after DMM) in different groups. **(F)** Quantification of bone mineral density and **(G)** bone volume of subchondral bone at late OA stages (total subchondral bone, 8 weeks and 12 weeks after DMM). Data are mean ± SD values, obtained from n = 5–8 animals in each group. One-way ANOVA followed by Bonferroni post hoc tests was performed to assess the significant difference between each group; $*p < 0.05$. **(H)** IHC staining of pSmad2/3 in subchondral bone in DMM-induced OA animals receiving different treatments. Representative IHC staining of pSmad2/3 in subchondral bone area of DMM-induced OA joints treated with PBS, PFD–PLGA + HA and commercial HA after 4 weeks and 12 weeks of DMM, with healthy joint as a control. Bar = 100 μm. **(I)** Quantification of pSmad2/3$^+$ cell density in subchondral bone zone (cell counts/mm^2) from IHC staining images. Data are mean ± SD values, obtained from n = 3–6 biological donors (n = 3 in healthy group; n = 6 in other groups). Two-way ANOVA, followed by Bonferroni post hoc tests was performed to assess the significant difference between each group.

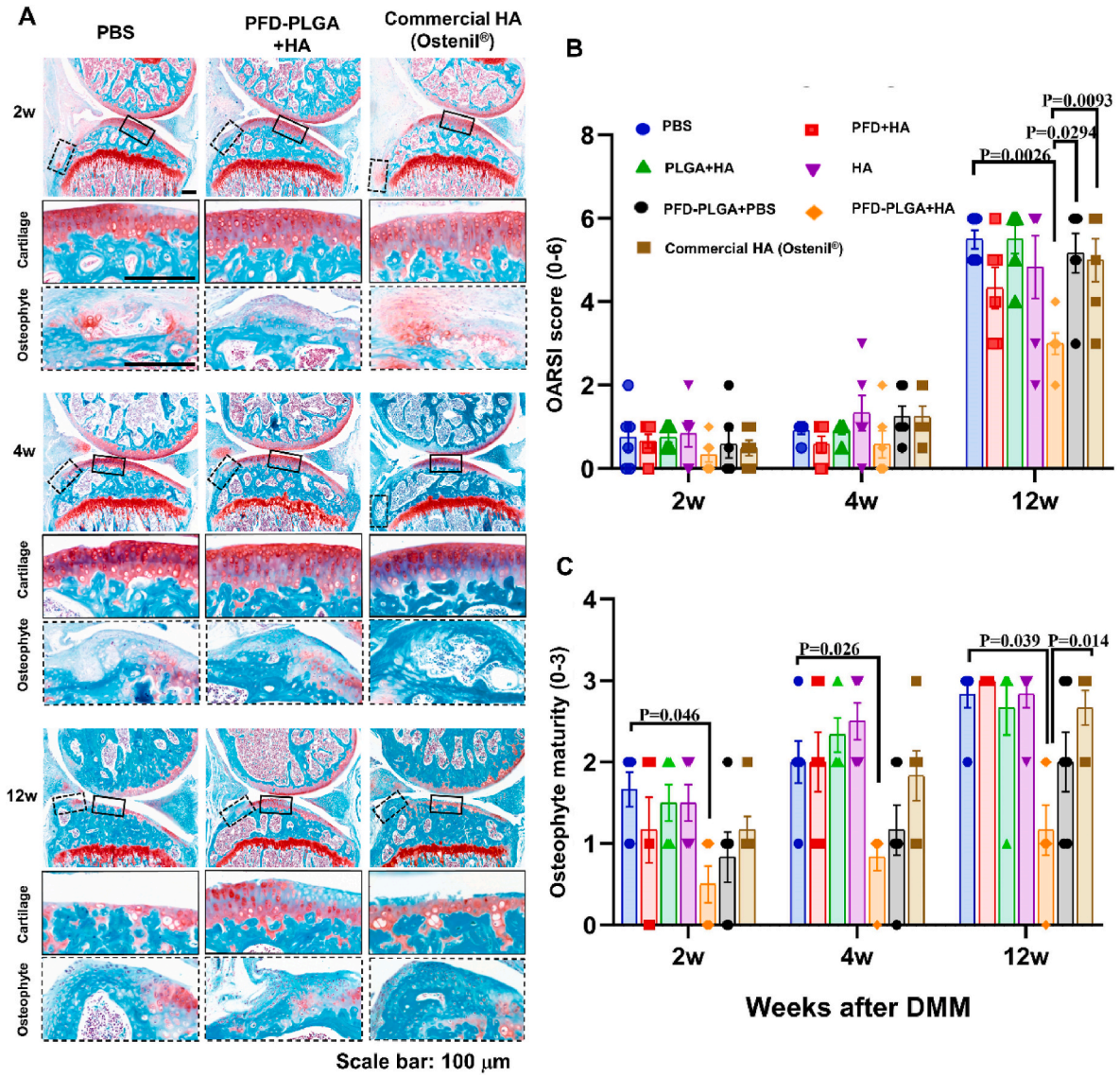

Fig. 4. Monthly I.A. injection of PFD–PLGA + HA attenuated cartilage degeneration and osteophyte maturity
A) Representative sagittal images of murine knee joints stained with Safranin O/Fast Green staining from PBS, PFD–PLGA + HA and commercial HA treatment groups at 2, 4, and 12 weeks after DMM. Enlarged structures of articular cartilage and osteophyte are in black boxes and dashed boxes; Scale bar = 100 μm. **(B)** Quantification results of joint degeneration in all treatment groups with modified OARSI score system. Data are mean ± SD values, n = 6 biological donors per group, and one-way ANOVA followed by Bonferroni post hoc tests was performed to assess the significant difference between each group. *p* values with significant difference ($p < 0.05$) are listed on the figure. **(C)** Quantification results of osteophyte maturity score of all treatment groups, detailed score system in Table S2. Data are mean ± SD values, obtained from n = 6 biological donors per group, and two-way ANOVA followed by Bonferroni post hoc tests was performed to assess the significant difference between each group, and *p* values with significant difference ($p < 0.05$) are listed on the figure.

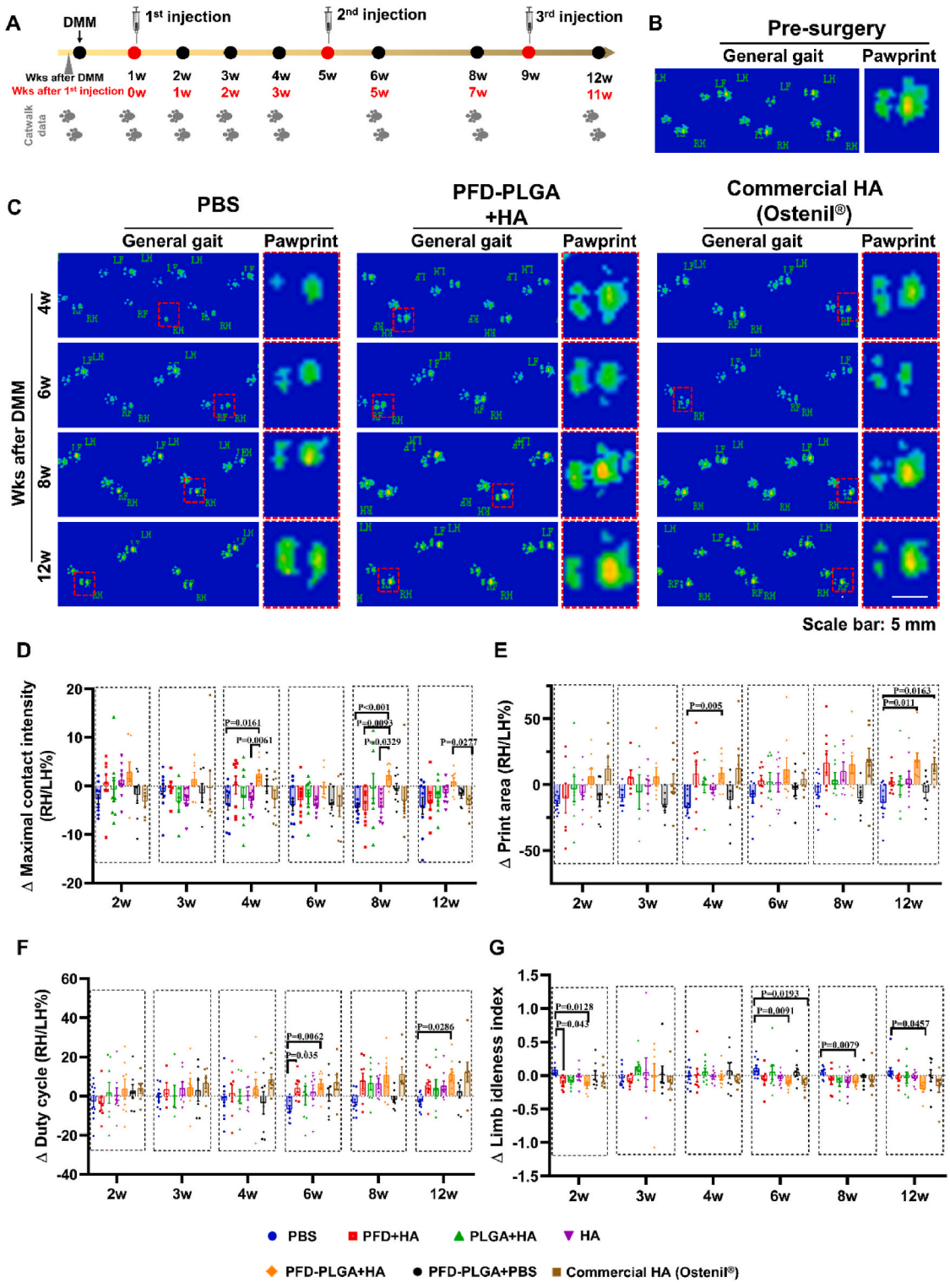

Fig. 5. Longitudinal evaluation of the pain-relief effect of PFD–PLGA + HA treatment during OA development

(A) Schematic diagram of study design and data collection. DMM surgery was performed on murine right knee joints, and monthly I.A. administration of different treatments at 1, 5 and 9 weeks after DMM. CatWalk data collection (footprints) at different timepoints is shown in the illustration. **(B)** Representative image of the gait and pawprints of mice with normal gait captured before DMM. **(C)** Representative image of murine gait and pawprint of PBS, PFD–PLGA + HA and commercial HA treatment groups at 4, 6, 8 and 12 weeks after DMM. Scale bar = 5 mm. **(D–G)** Time course analysis on gait parameters of **(D)** Δmaximal contact mean intensity (RH/LH, %), **(E)** Δmaximal contact area (RH/LH, %), **(F)** Δduty cycle(RH/LH, %), and **(G)** Δlimb idleness index (RH/LH, %) between different treatment groups (details in Table S1). Data are mean ± SD values, obtained from n = 6–8 animals per group, and a two-way ANOVA followed by Bonferroni post hoc tests was performed to assess the significant difference between each group at each timepoint. *p* values with significant difference ($p < 0.05$) are listed on the figure. RH: Right hind, LH: Left hind.

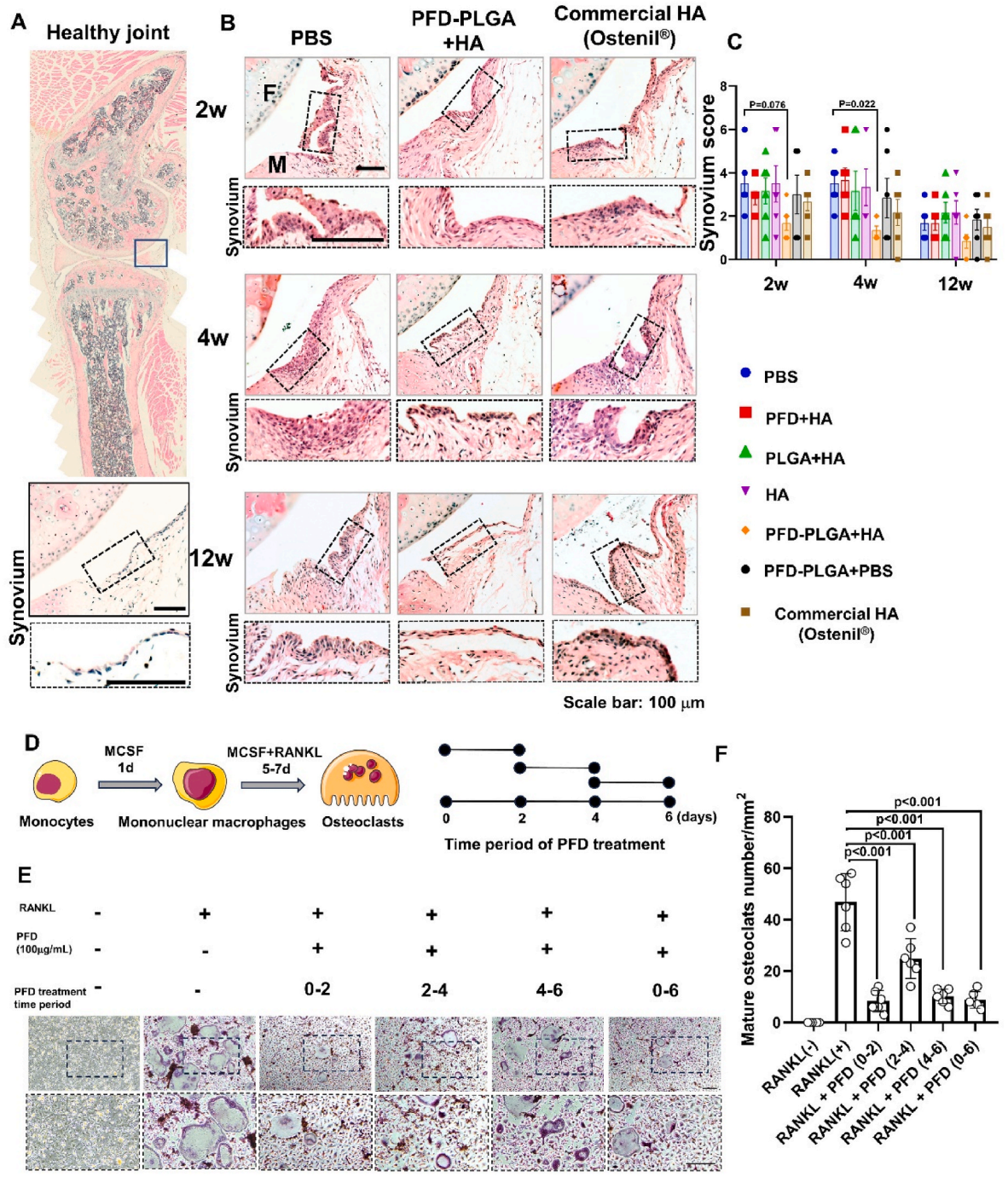

Fig. 6. PFD–PLGA + HA intervention attenuated synovitis in DMM-induced OA joints
(A) Representative H&E staining image of healthy synovium tissue adjacent to the medial meniscus (black box, the ROI selected in current study), and magnified images show the structure of non-inflamed synovial lining cells in the dashed box. Scale bar = 100 mm. **(B)** Representative images of synovium tissues of PBS, PFD–PLGA + HA and commercial HA treatment groups at 2, 4, and 12 weeks after DMM. The changes in the structure of synovial lining cells are shown in dashed boxes. Scale bar = 100 mm. **(C)** The severity of synovial inflammation and fibrosis was evaluated by synovitis score system (detailed scoring system in Table S3). Data are mean ± SD values, n = 6 animals per group; Each animal have 5 slides, and calculated by 3 ROIs under macroscope, statistical analysis was performed by one-way ANOVA followed by Bonferroni post hoc tests. **(D)**. PFD prohibited the differentiation and maturation of osteoclasts. Schematic diagram of osteoclasts differentiation and maturation (left panel) and PFD treatment time periods (right panel); **(E-F)**. Representative images of TRAP staining (**E**) for primary mouse osteoclast and the quantification of mature osteoclasts. Scale bar: 200 m. (**F**). Statistical analysis was performed using one-way ANOVA with Bonferroni post hoc test. N = 6 in each group.

3.9. Monthly I.A. Injection of PFD–PLGA + HA relieved synovitis and modulated the synovial macrophage polarization

To further understand the mechanism of pain relief effect of PFD–PLGA + HA treatment, we firstly examined the synovium histologically and histomorphometrically (Figs. 6 and 7). Synovium thickening is apparent in PBS group at 2 and 4 weeks after DMM surgery (Fig. 6A and B, dashed box), resulting in synovitis with high synovium scores (Fig. 6C; PBS group, 2 weeks, 3.500 ± 0.514; 4 weeks, 3.500 ± 0.391, respectively). Compared with the thicken synovium PBS group,

the PFD–PLGA + HA treatment group showed fewer lining cells in synovium (Fig. 6B, dashed box) with similar morphology in healthy joint (Fig. 6A), and the PFD–PLGA + HA treatment significantly relieved synovitis at 2 and 4 weeks after DMM (Fig. 6B). The synovium scores showed significant reduction in PFD–PLGA + HA treatment group at 4 weeks after DMM (Fig. 6, 4 weeks, PFD–PLGA + HA group, 1.333 ± 0.192 *vs.* PBS 3.500 ± 0.391, $p=0.022$).

Osteoclasts also play a key role in the progression of OA. We here also explored how PFD regulates osteoclast function *in vitro*. The osteoclast differentiation can be divided into different periods: the early phase (day 0–2), the middle phase (day 2–4), and the maturation phase (day 4–6) [35]. In order to investigate the roles of osteoclasts in different phases, we added PFD treatment at different time periods (early phase 0-2d, middle phase 2-4d, maturation phase 4-6d, and throughout the whole osteoclast differentiation phase 0-6d, Fig. 6D). The Trap staining results indicated that the PFD (100 μg/mL) can attenuate the early and middle osteoclast differentiation and the osteoclasts maturation ($p < 0.001$, Fig. 6E and F). Furthermore, the PFD treatment can also inhibit the osteoclast differentiation at all time points ($p < 0.001$, Fig. 6E and F).

Therefore, in the early stage of OA, the PFD-induced reduction of synovial inflammation (Fig. 6B and C) and osteoclastogenesis (Fig. 6D–F), and the maintenance of subchondral bone forming cells (Fig. 1F–H) possibly in together attenuates the early bone loss in subchondral bone.

As the anti-synovitis effect of PFD–PLGA + HA treatments may be partially attributed to the anti-inflammation property of PFD, we then checked the statues of synovial macrophages. Overall, in PFD–PLGA + HA treated mice, we found fewer total macrophages (Fig. 7A–C; F4/80$^+$ cells) and M1 macrophages (Fig. 7A–D; F4/80$^+$/iNOS$^+$ cells), more M2 macrophages (Fig. 7D and E; F4/80$^+$/CD206$^+$ cells) and thinner lining cells in synovium compared to other groups (Fig. 7A and B). Specifically, PBS and commercial HA treatment groups demonstrated significantly more synovial F4/80$^+$ pan-macrophages and iNOS$^+$ M1 macrophages at both 4 and 12 weeks after DMM (Fig. 7A–C, D). The ratio of synovial M2 macrophage to total macrophage increased in all DMM-induced OA knee joints compared to healthy non-injury joint (Fig. 7B–D). PFD–PLGA + HA treatment significantly reduced M1 synovial inflammatory macrophage infiltration at both 4 and 12 weeks after DMM compared to PBS group (Fig. 7A–D; iNOS$^+$ macrophage ratio in pan-macrophage: 4 weeks, PFD–PLGA + HA group, 44.97 ± 7.08 % *vs.* PBS group, 77.60 ± 4.61 %, $p=0.0028$; 12 weeks: PFD–PLGA + HA group 56.05 ± 2.87 % *vs.* PBS group 86.65 ± 4.90 %, $p=0.0357$). PFD–PLGA + HA treatment increased synovial M2 macrophage ratio significantly at 4 weeks after DMM (Fig. 7B–D; CD206$^+$ cell % in F4/80$^+$ cells: 4 weeks, 76.81 ± 4.42 % in PFD–PLGA + HA *vs.* 48.65 ± 16.02 % in PBS, $p=0.0311$), and no significant difference in M2 macrophage ratio was found between PBS, PFD–PLGA + HA, and commercial HA treated groups at 12 weeks after DMM.

To address the possible synergistic regulatory mechanism of PFD on macrophages and osteoblasts, we used condition media obtained from M0, M1 and M2 RAW264.7 macrophages after 48h of induction, and the macrophage condition medium was mixed with OM (1:1, vol/vol), and used to culture Saos-2 cells in the existence of TGFb1 (5 ng/mL). PFD (100 μg/mL) was added to the cultures to observe the regulatory effects in mineralization, and the readouts are the quantification of von kossa staining intensity after 14 days of culture (Fig. S8). From data we obtained, it is quite clear that PFD enhanced and rescued the mineralization of Saos-2 cells in the M1 and M2 condition medium groups, suggesting the regulating effect of PFD of Saos-2 mineralization under the influence of polarized macrophages. This data gives us more confidence that PFD could function in a macrophage activated environment, such as in OA joints.

To further investigate how PFD regulate the mineralization of Saos-2 and hBMSCs cells in TGFβ1 environment, we performed qPCR and growth factor (osteogenic and inflammatory factors) array assay to understand the expression levels of RNA and protein related to inflammation and osteogenic differentiation. The qPCR results indicated that under TGFβ1 treatment, PFD can enhance the gene expression of osteogenic differentiation marker (*i.e.* osteocalcin, Fig. S9A) and relieve the inflammation related maker (*i.e.* IL6, Fig. S9A). From the dot-plot results, we found that PFD did not change the osteogenic and inflammatory related markers in osteogenic medium without TGFβ1(5 ng/mL). When treated with TGFβ1 (5 ng/mL), the addition of PFD can enhance the osteogenic marker (OPG and osteoactivin, Fig. S9B), and inhibit inflammatory maker (IL-6, Fig. S9B).

These data demonstrate the anti-inflammatory and pro-osteogenesis effects of the PFD–PLGA + HA strategy in OA joints.

3.10. Monthly I.A. Injection of PFD–PLGA + HA mitigated pain through inhibiting calcitonin gene-related peptide (CGRP) in synovium and osteophytes

To further clarify the mechanism underlying the pain-relieving effect of PFD–PLGA + HA treatment, we examined the distribution of CGRP$^+$ cells in synovium and osteophytes (Fig. 8), as CGRP is a key OA pain transmitter neuropeptide.

The OA synovium displayed positive CGRP staining along the inflammatory zone (Fig. 8A), and compared with the healthy synovium, approximately 2.5 times more CGRP$^+$ cells were found in DMM-induced OA synovium at both 4 and 12 weeks after DMM (Fig. 8A; 4 weeks: PBS group, 66.21 ± 6.91 % *vs.* age-matched healthy joint, 18.86 ± 5.04 %, $p < 0.001$; 12 weeks: PBS group, 77.14 ± 14.35 cells/mm^2 *vs.* age-matched healthy joint, 17.35 ± 0.95 cells/mm^2, $p < 0.001$). A similar trend was found in the commercial HA group (Fig. 8A; 4 weeks: commercial HA, 71.33 ± 12.26 % *vs.* age-matched healthy joint, 18.86 ± 5.04 %, $p < 0.001$; 12 weeks: commercial HA, 76.79 ± 8.94 cells/mm^2 *vs.* healthy joint, 17.35 ± 0.95 %, $p < 0.001$). In the PFD–PLGA + HA treatment group, the CGRP$^+$ cells' percentage in synovium cells remained at a non-significant level, as in healthy knee joints (Fig. 8B; CGRP$^+$ cell number/total cell count in synovium, 4 weeks: PFD–PLGA + HA group, 34.00 ± 5.70 % *vs.* age-matched healthy control, 18.86 ± 5.04 %, $p > 0.990$; 12 weeks: PFD–PLGA + HA group, 43.24 ± 3.87 % *vs.* age-matched healthy control, 17.35 ± 0.97 %, $p=0.1432$). Specifically, compared with the non-treatment control (PBS group), PFD–PLGA + HA treatment significantly reduced the synovial CGRP $^+$ cell density at both 4 and 12 weeks after DMM (Fig. 8B; 4 weeks: PFD–PLGA + HA group, 34.00 ± 5.70 % *vs.* PBS, 66.21 ± 6.91 %, $p=0.0175$; 12 weeks: PFD–PLGA + HA group, 43.24 ± 3.87 % *vs.* PBS, 77.14 ± 14.35 %, $p=0.010$). Similarly, PFD–PLGA + HA treatment also reduced the synovial CGRP $^+$ cell density significantly when compared with commercial HA treatment (Fig. 8, 4 weeks: PFD–PLGA + HA, 34.00 ± 5.70 in *vs.* commercial HA, 71.33 ± 7.08, $p=0.0039$; 12 weeks: PFD–PLGA + HA, 43.24 ± 3.87 *vs.* commercial HA 76.79 ± 5.16, $p=0.011$).

The expression of CGRP in osteophytes was also assessed, as the presence of osteophytes is another cause of pain in OA joints [36]. The expression of CGRP in osteophytes was high in the PBS and commercial HA groups (Fig. 8C, dashed box), while that in the PFD–PLGA + HA group was significantly lower at both 4 and 12 weeks after DMM (Fig. 8C, dashed box). In addition, the percentage of CGRP$^+$ cells in osteophytes was significantly lower in the PFD–PLGA + HA group than in the PBS and commercial HA groups (Fig. 8D; 4 weeks: PFD–PLGA + HA, 22.80 ± 2.89 % *vs.* PBS, 42.24 ± 4.14 %, $p = 0.045$; PFD–PLGA + HA, 22.80 ± 2.89 % *vs.* commercial HA, 35.75 ± 16.36 %, $p = 0.067$; 12 weeks: PFD–PLGA + HA, 15.59 ± 5.72 % *vs.* PBS, 47.58 ± 3.71 %, $p = 0.036$; PFD–PLGA + HA, 15.59 ± 5.72 % *vs.* commercial HA, 44.06 ± 2.88 %, $p = 0.047$).

In summary, the sustained release of PFD using monthly I.A. injections of PFD–PLGA + HA successfully attenuated early OA phenotype in mice with DMM-induced OA knee joints by modulating the excessive TGFβ1-induced subchondral bone changes, in addition to exerting general disease-modifying effects such as relieving OA pain, preventing synovitis and osteophyte formation and maintaining joint cartilage

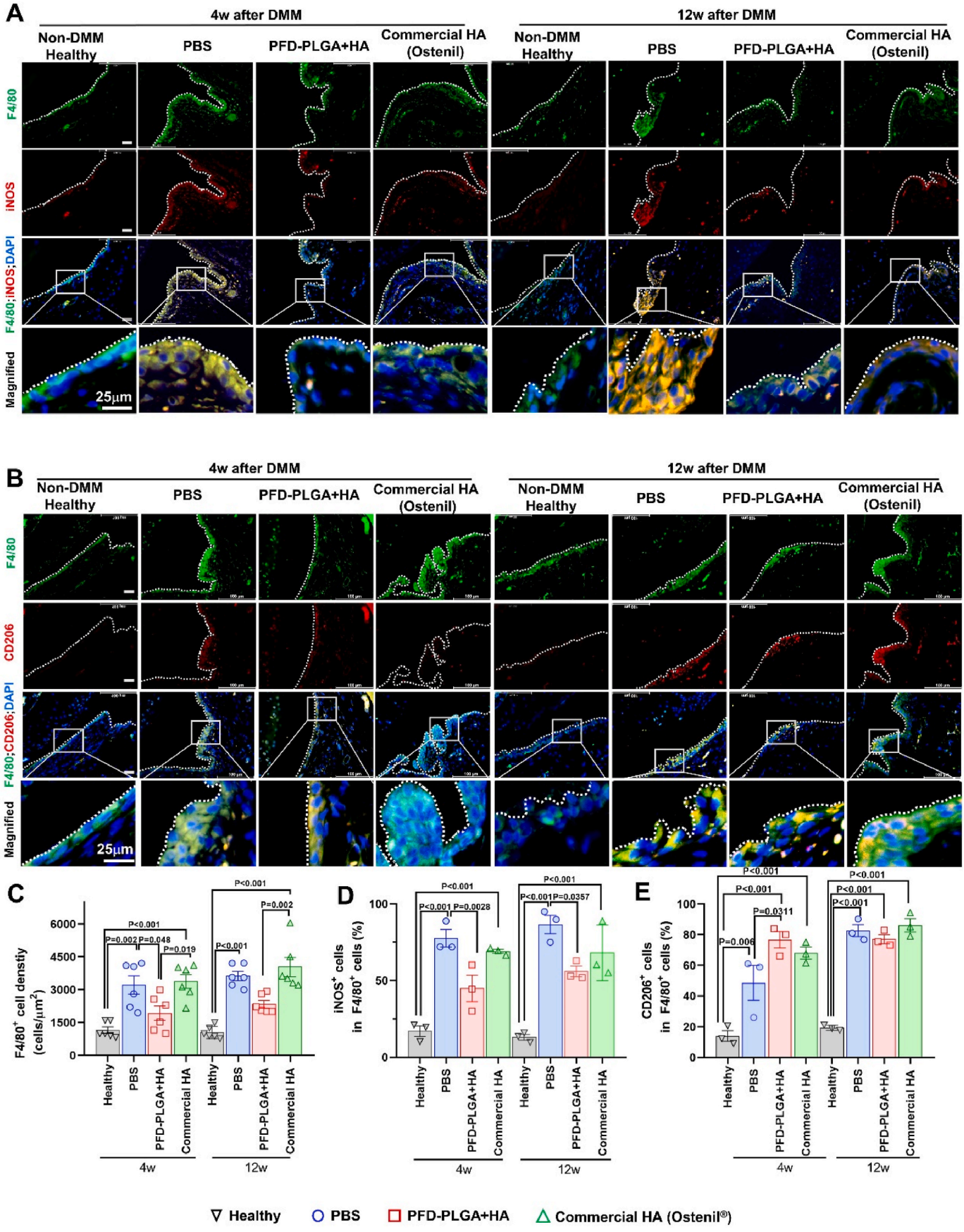

(caption on next page)

Fig. 7. PFD–PLGA + HA intervention re-polarized the M1 and M2 macrophages
(A) Representative immunofluorescent staining of M1 macrophages in mice synovium as the ROI indicated in Fig. 6A. The pan-macrophage marker F4/80 is stained green; M1 marker iNOS is stained red. The $iNOS^+$ (red) $F4/80^+$ (green) double stained areas were magnified in the lower panel, cell nuclei are stained blue by DAPI. Scale bar = 25 μm. **(B)** Representative immunofluorescent staining images of M2 macrophages in mice synovium. Pan-macrophage marker F4/80 is stained green; M2 marker CD206 is stained red. The $CD206^+$ (red) $F4/80^+$ (green) double stained areas were magnified in the lower panel, cell nuclei are stained blue by DAPI. Scale bar = 25 μm. **(C)** Quantification of the total macrophage density in mice synovium, counted by $F4/80^+$ cell number per synovium tissue area. **(D)** Proportion of M1 macrophage in the total macrophage, and **(E)** proportion of M2 macrophage in total macrophage. Data are mean ± SD values, and obtained from n = 3 animals per group. Each animal has 3 slides, and calculated by 3 ROIs under macroscope. Statistical analysis was performed by one-way ANOVA with Bonferroni post hoc test. *p* values with significant difference ($p < 0.05$) are listed on the figures.

homeostasis. Taken together, our results suggest that the PFD–PLGA + HA strategy has a high potential to serve as a novel DMOAD therapy for future clinical management of OA.

4. Discussion

Many recently developed OA drugs target articular cartilage, *e.g.*, small molecule SM04690 (targeting Wnt signaling) [37], sprifermin (targeting FGF18) [38], and UBX0101 (targeting senolytic signaling) [39]. However, these cartilage-targeting DMOADs show limited therapeutic effects in clinical trials. Here we demonstrated the feasibility of targeting aberrantly high levels of TGFβ1 in early-stage OA joints by using PFD to normalize the bone mineralization and protect the entire joint from OA progression without obvious side effect. Subchondral bone was selected as a major therapeutic target because subchondral bone undergoes dynamic changes prior to cartilage in the early stages of OA [40]. We observed the time-dependent phenotypic alterations of subchondral bone changes and found a rapid bone resorption at 1–4 weeks after DMM, and sclerosis development after 4 weeks post-DMM (Fig. 1A–D). The pathological changes in OA joints are mainly due to elevated levels of TGFβ1 locally. Not limited to the subchondral bone area, the overactivation of TGFβ signaling has been found in all type of tissues in OA joints [41]. Therefore, we aimed to target the overactivation of TGFβ1 signaling in early OA by I.A. delivery and sustained release of a TGFβ inhibitor, PFD, to prevent the subchondral bone changes in early-stage OA and prevent subsequent pathological progression.

As an anti-fibrotic drug for treating idiopathic pulmonary fibrosis and many other fibrosis diseases, PFD functions as a TGFβ inhibitor with anti-inflammatory effects [42]. We here first tested whether PFD could attenuate excessive TGFβ1-induced hypomineralization in bone-forming cells. The human osteoblastic cell line Saos-2 and hBMSCs were used as *in vitro* mineralization models to investigate the effect of PFD on TGFβ1 (Fig. 1E–H). PFD at concentrations of 0, 30, 100 and 500 μg/mL was tested in the presence of TGFβ1 at two pathological concentrations [2 and 5 ng/mL, as in human OA synovial fluid [43]]. We found that PFD at 100 μg/mL could rescue cell mineralization in a culture environment with excessive TGFβ (Fig. 1E–H). These *in vitro* results provide cellular-level evidence that PFD have the potential to rescue osteoblast hypomineralization and subchondral bone sclerosis in OA joints.

It is worth to mention that in clinical practice, patients with idiopathic pulmonary fibrosis take PFD orally at doses of 801–2403 mg/day. Most patients have to take oral PFD daily for more than 18 months, and the side effects include nausea, photosensitivity and gastrointestinal issues [44,45]. Considering the high incidence of side effects of systemic administration of PFD [27,46], and only a very low level of PFD is required at cellular level for subchondral bone remodeling (100 μg/mL, Fig. 1E–H), the next question is how to maintain the identified effective dose of PFD in OA joints and can reach subchondral bone, we therefore designed the local long-term drug release method, namely, the "PFD–PLGA + HA" strategy (Fig. 3A).

Our considerations in designing this "PFD–PLGA + HA" strategy included: (**1**) using I.A. administration to avoid gastrointestinal side effects; (**2**) lowering the administration frequency, *i.e.*, PFD was sustainably released at a low dose (100 μg/mL, Fig. 1) for up to 4 weeks (Fig. 2) by using the biodegradable polymer PLGA; and (**3**) increasing the retention of drug-loaded PLGA-MS and the drug released from PLGA-MS in the joint cavity; for this, PFD–PLGA-MS was dissolved in an HA solution at a clinically applied concentration (1.5 %) and molecular weight (1500 kDa). All above elements together formed a complete monthly I.A. injection "PFD–PLGA + HA" strategy. Following this design, we achieved sustained release of PFD in early-OA knee joints with enhanced both safety and therapeutic effects, and significantly simplified the administration procedure (Fig. 3A).

From the cell study, we optimized that PFD at 100 μg/mL is effective for rescuing the mineralization of bone forming cells (Fig. 1 F–H). We then aimed to keep this concentration in joint cavity as long as we could, thus designed the release system by adjusting the PFD loading dosage and PLGA system. To achieve this, we dissolved 1 mg PFD-loaded PLGA MS in 1 mL PBS or HA for *in vivo* injection. According to the PFD loading efficacy (192 μg/mg MS), we injected 10 μL (1.92 μg PFD) PFD-PLGA MS solution into each mice knee joint. Considering that there are only 1.2–6.2 μL synovial fluid in mice knee joint, the final concentration of the PFD varied from 118.5 to 171.4 μg/mL, which is within the effective concentration of our *in vitro* test. We believe this certain set-up is stable and can be scale up to large animals and human by simply amplify the volume of solution for I.A. injections without change of concentration. Considering the synovial fluid volume in human joint is ~6.7 mL per joint, for the future transition to humans with the mimic the *in vitro* working concentration of PFD (~100 μg/mL) and the loading efficacy, the estimated average volume of injection solution (1 mg MS/mL) is around 7.3 mL, and the according amount of the microsphere is 7.3 mg, therefore the total PFD of single injection is around 1398.26 μg by estimated calculation. We would like to take this chance to address the safety of this strategy by mentioning the following numbers again: in the case of treating patients with idiopathic pulmonary fibrosis, the recommended oral application dosage of PFD for maintaining a stable and effective concentration in the plasma is 801 mg per serve, three times daily (i.e., 2403 mg per day). In our case, we are expecting therapeutic effects by single I.A. injection of ~1.4 mg PFD contented PLGA particles in HA, and the effects are expecting to last for 30 days, this is significantly lower compared to the current clinical drug administration method.

Hydrogel-based microsphere or microneedle (*i.e.,* hyaluronic acid methacrylate, chitosan, Alginate HA, GelMa etc.) system are currently developed as a carrier for DMOADs [47–49]. Regarding the clearance of PLGA particles in joint, we think HA is very important for the PLGA microspheres retention. In the animal study, we have set a PFD-loaded PLGA MS group as control (PFD-PLGA + PBS group in Figs. 3–6), and we did not observe any therapeutic effects in the PFD-PLGA MS group, which reflect a fast naturally drainage of the PLGA particles from the joint, most likely before the degradation. The joint retention of PLGA particle in the comprehensive system is attributed to HA. If considering the future application in humans, it is possible that the microspheres could be cleared from the joint in 4 weeks, this is based on the estimation of *in vivo* tracing data at day 28, we observed 0.85 % of the ICG signal intensity compared to day 0 (Fig. 2H–J).

Our results demonstrated that exposure to PFD had an immediate pain relief effect in the first week after injection (groups of PFD + HA, PFD-PLGA + HA; Figs. 3, 5 and 8), and synovitis was well controlled in the early inflammation stages with a single injection (2 and 4 weeks after DMM, Figs. 3A, 5 and 8), supporting the function of PFD on

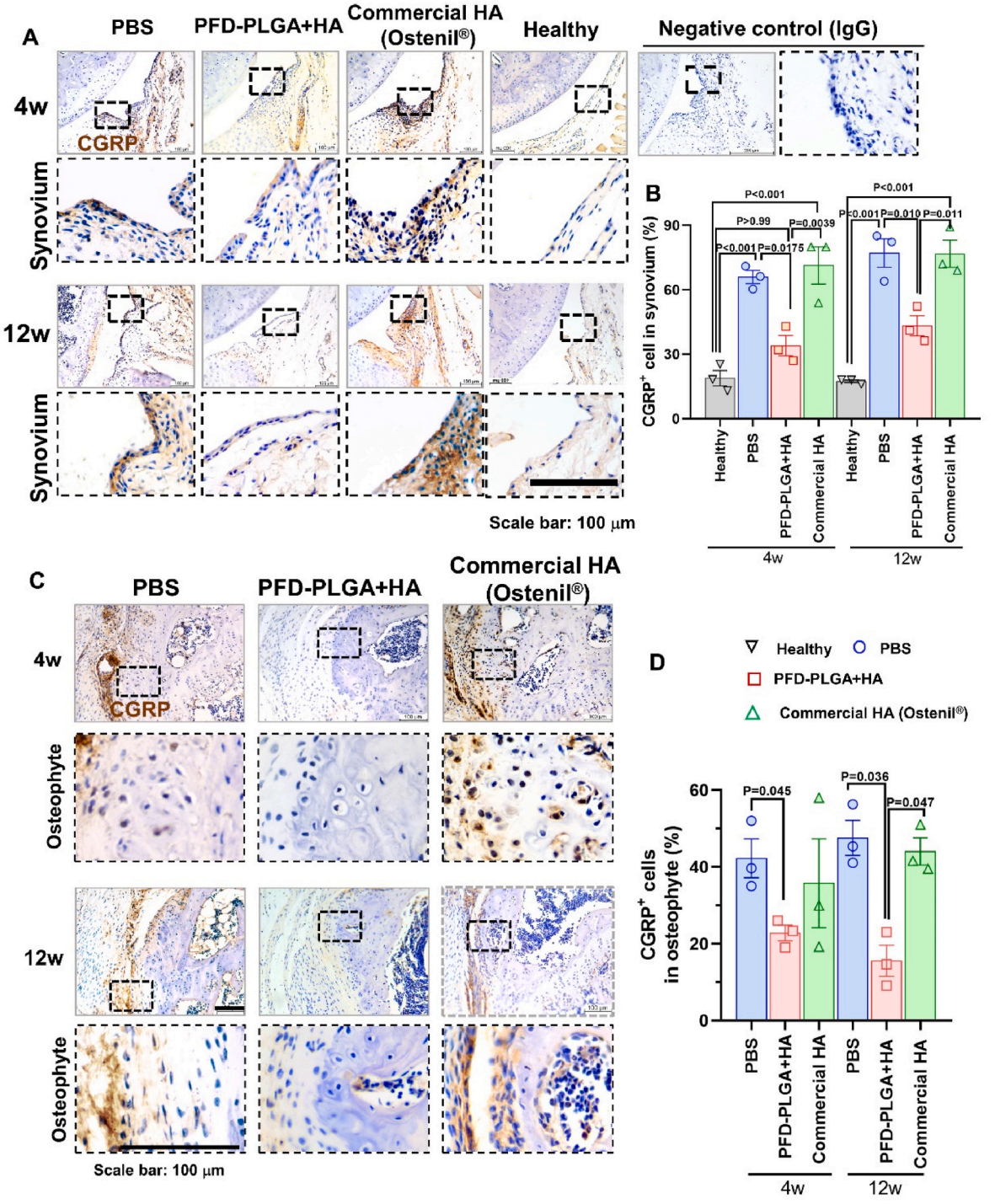

Fig. 8. PFD–PLGA + HA treatment reduced joint pain by attenuating synovial and osteophytic CGRP
(A) Representative IHC staining of CGRP in the mouse synovium from the PBS, PFD–PLGA + HA and commercial HA (Ostenil®) groups at 4 and 12 weeks after DMM. The ROI selection is indicated in Fig. 6A, and the CGRP positive signal is brown. The magnified areas were highlighted in the dashed box. Right panel shows uninjured joints (healthy) and negative stained controls (IgG). Scale bar = 100 μm. **(B)** Ratio of $CGRP^+$ cells in total synoviocytes. Data presented as means ± SD, obtained from n = 3 animals in each group. Each animal 3 slides, and calculated by 3 ROIs under macroscope,. Statistical analysis was performed using Kruskal-Wallis test. *p* values are listed. **(C)** Representative IHC staining of CGRP in mice osteophytes from PBS, PFD–PLGA + HA and Commercial HA (Ostenil®) groups at 4 and 12 weeks after DMM. The magnified areas were highlighted by the dashed box. Scale bar = 100 μm. **(D)** Ratio of $CGRP^+$ cells in osteophytes. Data presented as means ± SD, obtained from n = 3 animals in each group. Each animal 3 slides, and calculated by 3 ROIs under a macroscope. Statistical analysis was performed using Kruskal-Wallis test. *p* values with significant difference ($p < 0.05$) are listed on the figure.

synovium like Wei et al. reported in rabbits [26]. Meanwhile, the pain relief effect was not significant in PFD-PLGA + PBS group, suggesting that HA is critical to keep the drug-loaded MS and local PFD concentration in joint cavity (Fig. 5); the drug-loaded MS is most likely be rapidly eliminated *via* the synovial lymphatic system in the absence of HA [31]. Thus, HA is indispensable in this design; its lubricative effects is not the main consideration, but an additional function. We too compared our strategy with current clinical HA treatment (commercial

HA). Surprisingly, monthly I.A. injection of "PFD–PLGA + HA" has overall pain relief, symptom-relieving effects, and also demonstrated multitarget disease-modifying effects: it regulated multiple tissues in OA joints, namely, subchondral bone (Fig. 3), cartilage (Fig. 4) and the synovium (Figs. 6–8), and its influence runs through all stages of OA development. We believe that the following aspects made this therapeutic strategy more effective: as a TGFβ1 inhibitor, PFD firstly acted on the synovium and cartilage after being released from PLGA-MS, and the low level of PFD was jointly maintained by PLGA and HA in joint cavity, and spread to subchondral bone, thus regulating subchondral bone in the long term.

Like predicted in the cell-based study (Fig. 1), we observed subchondral bone remodeling effects of PFD–PLGA + HA treatment in OA animals, and our results showed subchondral bone-modulating effects in all stages of OA. Specifically, it maintained the subchondral bone phenotype and density in both early OA and late OA stages, and successfully prevented the excessive TGFβ1-incurred subchondral bone loss in early OA and sclerosis in late OA (Fig. 3A–G). We also observed less osteophytes and reduced joint pain (Figs. 4A and 5), and less synovial and osteophytic CGRP expression (Fig. 8), which are the histological features for pain relief effect. We believe that the PFD released from PLGA effectively acted on bony tissues under the cartilage, which can be supported by the lower expression levels of subchondral pSmad2/3, the markers of TGFβ-signaling activation observed in the PFD–PLGA + HA group, compared with the PBS and commercial HA groups (Fig. 3H). The route by which free PFD reached subchondral bone may be through inherent small channels in joint tissue. This could be supported by a cadaveric study that peri-entheseal vascular structure accumulation in anterior and posterior cruciate ligaments (ACL and PCL, respectively) in both healthy and OA knee by histology and magnetic resonance imaging assessments [50]. These peri-entheseal vascular structures in the ACL and PCL were correlated with distribution of peri-entheseal bony pathological changes (*e.g.,* bone marrow lesion) [50].

In terms of the cellular and molecular mechanism of PFD's effect on OA joints, the PFD–PLGA + HA treatment showed immunoregulatory effects on joint tissues and reduced M1 macrophage infiltration throughout all stages of OA (Fig. 7), and elevated numbers of M2 macrophages were only seen in early-stage OA (4 weeks after DMM, Fig. 7), but not in the late stage. Recently, Li et al., designed an M1 macrophage-targeted nanomicelle-hydrogel microsphere, which is fabricated by dexamethasone (DEX)-loaded nanomicelles and GelMa *via* microfluidic technology [51], and can accurately bind to M1 macrophages to promote M1 macrophage apoptosis and induce M1 polarization inhibition [51]. Similarly, our delivery system also showed the inhibitory effects of M1 macrophages. Further, given that M2 macrophages have been proved to be correlated with tissue fibrosis at late stage of OA, our intervention not only exerted anti-inflammatory effects but also protected against further synovial fibrosis. Similarly, there is research evidence for the anti-inflammatory and anti-fibrotic effects of PFD in synovial fibroblasts. A previous study showed that PFD at 1 mg/mL reduced the expression of Col1a1 and IL-6 in human synovium-derived fibroblasts and inhibited fibroblast proliferation *in vitro* [26]. It is possible that PFD provides cartilage protection by both inhibiting IL-1β signaling and reducing the production of MMP and other inflammatory cytokines, because PFD has also been shown to exert its anti-inflammatory effect *via* inhibiting the production of MMP and inflammatory cytokines such as TNFα, IL-1β, IL-6 and IL-8, which could also attenuate the MMP-induced cartilage degeneration [23,52], and this also can be supported by a study by Benton et al., who demonstrated that PFD (0–5 μM) did not affect cartilage matrix balance and inhibited the IL-1β-induced nitric oxide release in a dose-dependent manner in cell culture models [53].

Taken together, we observed overall pain relief, symptom-relieving effects and disease-modifying effects in multiple joint tissues in the monthly PFD–PLGA + HA treatment groups, including subchondral bone, cartilage and the synovium, in the experimental animals (Figs. 3–8). Last but not least, we need to emphasis again on the safety and long-term pain relief effect of this strategy. The ability to achieve long-term pain relief using monthly I.A. injection along has great potential to address the significant clinical need for pain management in patients with OA. In addtion, all elements involved in this strategy are FDA-approved and have been used in clinical for many years, and the much lower dosage (less than 1/1000 compared to oral administration) and frequency (monthly injection compared to daily administration) of administration would not cause additional safety concerns during clinical translation.

The current study has limitations. First, we did not apply the PFD–PLGA + HA treatment to aging related spontaneous OA model and large OA animal models such as porcine or equine. These animal models recapitulate the most common cases of human OA. Further investigation will be conducted in aging related models and large animal models. In addition, we did not apply the I.A. injection in established OA model (*i.e.,* 8/12 weeks after DMM) to assess the therapeutic effects of the intervention for reversing OA, and future assessment of the attenuative effects of the PFD-PLGA MS for reversing OA are in need. Second, it is difficult to trace the drug *in vivo*. We cannot directly label the PFD molecule with fluorescent tags because these tags have a higher molecular weight than PFD, but the significantly lower expression levels of pSMAD2/3 indicted a lower level of TGFβ-signaling activation in PFD–PLGA + HA treatment group, which partially supported the effectiveness of PFD on subchondral bone. Third, there might be gender differences that have yet to be investigated. We evaluated the effects of PFD on mineralization by Saos-2 cell and hBMSCs *in vitro*. Saos-2 cells were derived from female patients, and the hBMSCs were isolated from three female patients due to the availability of cell lines in the laboratory, and only male mice were used for the DMM model to avoid the hormonal effects [54]. But overall, the therapeutic effects of PFD were confirmed cross multiple assays. Further pre-clinical and clinical trials will also be conducted to evaluate the effectiveness and include both genders.

In conclusion, this long-term release system of PFD attenuated subchondral bone pathology, osteophyte formation, pain-related behavioral alterations, and alleviated OA phenotype, indicating its potential to be a novel therapeutic strategy for OA treatment. To our knowledge, this is the first report about I.A. sustained-release of PFD as a disease-modifying treatment for early OA, and this strategy has high potential to become the next generation of DMOAD therapy.

5. Experimental section

5.1. Study design

The goal of this study was to halt early OA development, particularly the subchondral bone changes, by targeting the excessive amount of TGFβ at the target site by controlled release of a clinically approved TGFβ inhibitor, PFD. Our initial *in vitro* studies were performed in Saos2 cells and primary hBMSCs to examine the effect of PFD treatment on osteoblast-like mineralization in the presence of high levels of TGFβ in the culture medium (Fig. 1E). To achieve *in vivo* long-term controlled release of PFD in the OA joint cavity at an effective dose, we encapsulated PFD in PLGA and manufactured microparticles, and injected these microparticles into OA joints together with clinically used HA (the "PFD–PLGA + HA" strategy, Fig. 3A). OA animal models were established by subjecting mice to DMM surgery, and these models were treated once a month with our treatment strategy (Fig. 3A–Table S1). To evaluate OA progression, histology, OARSI scoring, gait analysis and immunostaining of specific cellular and molecular targets were conducted, and the observers performing the analysis were blinded to whether the samples were from treated or control animals. All results of the *in vitro* study were analyzed *via* conventional laboratory readouts. De-identified human bone marrow stem cells were isolated from the femoral head of patients undergoing total hip arthroplasty, and their

tissue samples were collected with ethical approval from the Joint Chinese University of Hong Kong-New Territories East Cluster Clinical Research Ethics Committee (CUHK-NTEC Ref. No. 2013.248 and Ref. No. 2019.078). All animal experiments were conducted following the "Animal Research: Reporting of *in vivo* Experiments" guidelines, and animals' care was in accordance with CUHK guidelines. For experiments expected to yield large differences, the standard practice of using five to eight replicates was followed. Sample sizes, biological replicates and statistical methods are provided in the corresponding figure legends. No data were excluded from analysis.

Ethics approval and consent to participate

Human tissue samples were collected with ethical approval from the Joint Chinese University of Hong Kong-New Territories East Cluster Clinical Research Ethics Committee (CUHK-NTEC Ref. No. 2013.248 and Ref. No. 2019.078). All signed consent statement form were collected and recorded.

All animal experiments were conducted following the "Animal Research: Reporting of *in vivo* Experiments" guidelines, and animals' care was in accordance with the guidelines of the Chinese University of Hong Kong (CUHK, Shatin, Hong Kong SAR). The experimental design was reviewed and approved by the university's Animal Ethics and Experimental Committee (Reference No. 19-241-MIS, No. 22-333-GRF).

CRediT authorship contribution statement

Xiaobo Zhu: Writing – original draft, Visualization, Validation, Methodology, Investigation, Formal analysis, Data curation. **Mingde Cao:** Methodology, Investigation. **Kejia Li:** Validation, Investigation. **Yau-Tsz Chan:** Validation, Methodology, Investigation. **Hon-Fai Chan:** Supervision, Methodology, Investigation, Funding acquisition. **Yi-Wah Mak:** Supervision, Methodology. **Hao Yao:** Supervision, Methodology. **Jing Sun:** Validation, Investigation. **Michael Tim-Yun Ong:** Supervision, Resources, Methodology. **Kevin Ki-Wai Ho:** Resources, Methodology. **Chien-Wei Lee:** Supervision, Resources, Methodology. **Oscar Kuang-Sheng Lee:** Supervision, Resources, Methodology. **Patrick Shu-Hang Yung:** Supervision, Resources, Methodology, Funding acquisition. **Yangzi Jiang:** Writing – review & editing, Writing – original draft, Visualization, Validation, Supervision, Resources, Project administration, Methodology, Investigation, Funding acquisition, Formal analysis, Data curation, Conceptualization.

Declaration of competing interest

Y.J. and X.Z. are the inventors on patent application (US App No. 63/362,181; CN App. No. 202211342741.9; PCT/CN2022/128506; EU App. No. 22934779.4) submitted by the Chinese University of Hong Kong. All other authors declare no competing interests.

Acknowledgements

All authors appreciated the technical support from the core facilities in the School of Biomedical Science and Department of Orthopaedics and Traumatology, the Chinese University of Hong Kong. We would like to specifically thank Dr. Bruma Sai Chuen Fu for his suggestions on methodology and data analysis, and Prof. Rocky Tuan for kind comments. The Saos2 cell line was kindly gifted by Dr. Carol Lau from Department of Orthopaedic and Traumatology, the Chinese University of Hong Kong. We sincerely thank all the supports from all parties during the Covid-19 pandemic. The project was supported by (1) the National Key R&D Program of China (Project No. 2019YFA0111900 to YJ), which is financed by the Ministry of Science and Technology of the People's Republic of China (MOST, China); (2) this work described in this paper was partially supported by a grant from the NSFC/RGC Joint Research Scheme sponsored by the Research Grants Council of the Hong Kong Special Administrative Region, China and the National Natural Science Foundation of China (Project No. N_CUHK483/22 to YJ); (3) the Center for Neuromusculoskeletal Restorative Medicine [CNRM at InnoHK, to YJ, HC, PY] by Innovation and Technology Commission (ITC) of Hong Kong SAR, China; (4) the Natural Science Foundation of China (Project No 82302728 to XZ); (5) The Chinese University of Hong Kong.

Appendix A. Supplementary data

Supplementary data to this article can be found online at https://doi.org/10.1016/j.bioactmat.2024.05.028.

References

[1] H. Long, Q. Liu, Y. Zhang, A. Guo, J. Lin, Prevalence estimates of osteoarthritis from Global Burden of disease study 2019, Arthritis Rheumatol. (2022), https://doi.org/10.1002/art.42134.

[2] D.J. Hunter, S. Bierma-Zeinstra, Osteoarthritis, Lancet 393 (2019) 1745–1759, https://doi.org/10.1016/S0140-6736(19)30417-9.

[3] R. Geenen, C.L. Overman, R. Christensen, P. Åsenlöf, S. Capela, K.L. Huisinga, M.E. P. Husebø, A.J.A. Köke, Z. Paskins, I.A. Pitsillidou, C. Savel, J. Austin, A.L. Hassett, G. Severijns, M. Stoffer-Marx, J.W.S. Vlaeyen, C. Fernández-De-Las-Peñas, S. J. Ryan, S. Bergman, EULAR recommendations for the health professional's approach to pain management in inflammatory arthritis and osteoarthritis, Ann. Rheum. Dis. 77 (2018) 797–807, https://doi.org/10.1136/annrheumdis-2017-212662.

[4] R.R. Bannuru, M.C. Osani, E.E. Vaysbrot, N.K. Arden, K. Bennell, S.M.A. Bierma-Zeinstra, V.B. Kraus, L.S. Lohmander, J.H. Abbott, M. Bhandari, F.J. Blanco, R. Espinosa, I.K. Haugen, J. Lin, L.A. Mandl, E. Moilanen, N. Nakamura, L. Snyder-Mackler, T. Trojian, M. Underwood, T.E. McAlindon, OARSI guidelines for the non-surgical management of knee, hip, and polyarticular osteoarthritis, Osteoarthr. Cartil. 27 (2019) 1578–1589, https://doi.org/10.1016/j.joca.2019.06.011.

[5] A. Jørgensen, K. Stengaard-Pedersen, O. Simonsen, M. Pfeiffer-Jensen, C. Eriksen, H. Bliddal, N.W. Pedersen, S. Bødtker, K. Hørslev-Petersen, L.Ø. Snerum, N. Egund, H. Frimer-Larsen, Intra-articular hyaluronan is without clinical effect in knee osteoarthritis: a multicentre, randomised, placebo-controlled, double-blind study of 337 patients followed for 1 year, Ann. Rheum. Dis. 69 (2010) 1097–1102, https://doi.org/10.1136/ard.2009.118042.

[6] A. Gazendam, S. Ekhtiari, A. Bozzo, M. Phillips, M. Bhandari, Intra-articular saline injection is as effective as corticosteroids, platelet-rich plasma and hyaluronic acid for hip osteoarthritis pain: a systematic review and network meta-analysis of randomised controlled trials, Br. J. Sports Med. 55 (2021) 256–261, https://doi.org/10.1136/bjsports-2020-102179.

[7] T. V Pereira, P. Jüni, P. Saadat, D. Xing, L. Yao, P. Bobos, A. Agarwal, C. A. Hincapié, B.R. da Costa, Viscosupplementation for knee osteoarthritis: systematic review and meta-analysis, BMJ (2022) e069722, https://doi.org/10.1136/bmj-2022-069722.

[8] J. Shen, S. Li, D. Chen, TGF-β signaling and the development of osteoarthritis, Bone Res 2 (2014), https://doi.org/10.1038/boneres.2014.2.

[9] D. Muratovic, D.M. Findlay, F.M. Cicuttini, A.E. Wluka, Y.R. Lee, S. Edwards, J. S. Kuliwaba, Bone marrow lesions in knee osteoarthritis: regional differences in tibial subchondral bone microstructure and their association with cartilage degeneration, Osteoarthr. Cartil. 27 (2019) 1653–1662, https://doi.org/10.1016/j.joca.2019.07.004.

[10] D. Muratovic, D.M. Findlay, R.D. Quarrington, X. Cao, L.B. Solomon, G.J. Atkins, J. S. Kuliwaba, Elevated levels of active Transforming Growth Factor β1 in the subchondral bone relate spatially to cartilage loss and impaired bone quality in human knee osteoarthritis, Osteoarthr. Cartil. 1 (2022) 1–12, https://doi.org/10.1016/j.joca.2022.03.004.

[11] S. Hering, F. Isken, C. Knabbe, J. Janott, C. Jost, A. Pommer, G. Muhr, H. Schatz, A. Pfeiffer, TGF β 1 and TGF β 2 mRNA and protein expression in human bone samples, Exp. Clin. Endocrinol. Diabetes 109 (2001) 217–226, https://doi.org/10.1055/s-2001-15109.

[12] Y. Okamoto, Y. Gotoh, O. Uemura, S. Tanaka, T. Ando, M. Nishida, Age-dependent decrease in Serum transforming growth factor (TGF)-Beta 1 in healthy Japanese individuals; Population study of Serum TGF-beta 1 level in Japanese, Dis. Markers 21 (2005) 71–74, https://doi.org/10.1155/2005/381215.

[13] J. Geurts, A. Patel, M.T. Hirschmann, G.I. Pagenstert, M. Müller-Gerbl, V. Valderrabano, T. Hügle, Elevated marrow inflammatory cells and osteoclasts in subchondral osteosclerosis in human knee osteoarthritis, J. Orthop. Res. 34 (2016) 262–269, https://doi.org/10.1002/jor.23009.

[14] R.K. Zhang, G.W. Li, C. Zeng, C.X. Lin, L.S. Huang, G.X. Huang, C. Zhao, S.Y. Feng, H. Fang, Mechanical stress contributes to osteoarthritis development through the activation of transforming growth factor beta 1 (TGF-β1), Bone Jt, Res. 7 (2018) 587–594, https://doi.org/10.1302/2046-3758.711.BJR-2018-0057.R1.

[15] Z. Cui, J. Crane, H. Xie, X. Jin, G. Zhen, C. Li, L. Xie, L. Wang, Q. Bian, T. Qiu, M. Wan, M. Xie, S. Ding, B. Yu, X. Cao, Halofuginone attenuates osteoarthritis by inhibition of TGF-β activity and H-type vessel formation in subchondral bone, Ann. Rheum. Dis. 75 (2016) 1714–1721, https://doi.org/10.1136/annrheumdis-2015-207923.

[16] Y. Li, W. Mu, B. Xu, J. Ren, T. Wahafu, S. Wuermanbieke, H. Ma, H. Gao, Y. Liu, K. Zhang, A. Amat, L. Cao, Artesunate, an anti-Malaria agent, attenuates

experimental osteoarthritis by inhibiting bone resorption and CD31hiEmcnhi vessel formation in subchondral bone, Front. Pharmacol. 10 (2019), https://doi.org/10.3389/fphar.2019.00685.
[17] G. Zhen, C. Wen, X. Jia, Y. Li, J.L. Crane, S.C. Mears, F.B. Askin, F.J. Frassica, W. Chang, J. Yao, J.A. Carrino, A. Cosgarea, D. Artemov, Q. Chen, Z. Zhao, X. Zhou, L. Riley, P. Sponseller, M. Wan, W.W. Lu, X. Cao, Inhibition of TGF-β signaling in mesenchymal stem cells of subchondral bone attenuates osteoarthritis, Nat. Med. 19 (2013) 704–712, https://doi.org/10.1038/nm.3143.
[18] L. Xie, F. Tintani, X. Wang, F. Li, G. Zhen, T. Qiu, M. Wan, J. Crane, Q. Chen, X. Cao, Systemic neutralization of TGF-β attenuates osteoarthritis, Ann. N. Y. Acad. Sci. 1376 (2016) 53–64, https://doi.org/10.1111/nyas.13000.
[19] R. Chen, M. Mian, M. Fu, J.Y. Zhao, L. Yang, Y. Li, L. Xu, Attenuation of the progression of articular cartilage degeneration by inhibition of TGF-β1 signaling in a mouse model of osteoarthritis, Am. J. Pathol. 185 (2015) 2875–2885, https://doi.org/10.1016/j.ajpath.2015.07.003.
[20] L. Richeldi, U. Yasothan, P. Kirkpatrick, Pirfenidone, Nat. Rev. Drug Discov. 10 (2011) 489–490, https://doi.org/10.1038/nrd3495.
[21] S.M. Ruwanpura, B.J. Thomas, P.G. Bardin, Pirfenidone: molecular mechanisms and potential clinical applications in lung disease, Am. J. Respir. Cell Mol. Biol. 62 (2020) 413–422, https://doi.org/10.1165/rcmb.2019-0328TR.
[22] J.J. Solomon, S.K. Danoff, F.A. Woodhead, S. Hurwitz, R. Maurer, I. Glaspole, P. F. Dellaripa, B. Gooptu, R. Vassallo, P.G. Cox, K.R. Flaherty, H.I. Adamali, M. A. Gibbons, L. Troy, I.A. Forrest, J.A. Lasky, L.G. Spencer, J. Golden, M. B. Scholand, N. Chaudhuri, M.A. Perrella, D.A. Lynch, D.C. Chambers, M. Kolb, C. Spino, G. Raghu, H.J. Goldberg, I.O. Rosas, S. Haynes-Harp, F. Poli, C.S. Vidya, R.R. Baron, T. Clouser, T. Doyle, A. Maeda, K.B. Highland, J.F. Albayda, S. E. Collins, K.S. Suresh, J.M. Davis, A.H. Limper, I. Amigues, K. Eliopoulos, J. J. Swigris, S. Humphries, J.C. Huntwork, C. Glynn, S.R. Duncan, M.I. Danila, M. K. Glassberg, E.M. Oberstein, E.A. Belloli, L. Briggs, V. Nagaraja, L. Cholewa, D. DiFranco, E. Green, C. Liffick, T. Naik, G. Montas, D. Lebiedz-Odrobina, R. Bissell, M. Wener, L.H. Lancaster, L.J. Crawford, K. Chan, R.J. Kaner, A. Morris, X. Wu, N.A. Khalidi, C.J. Ryerson, A.W. Wong, C.D. Fell, S.A. LeClercq, M. Hyman, S. Shapera, S. Mittoo, S. Shaffu, K. Gaffney, A.M. Wilson, S. Barratt, H. Gunawardena, R.K. Hoyles, J. David, N. Kewalramani, T.M. Maher, P. L. Molyneaux, M.A. Kokosi, M.J. Cates, M. Mandizha, A. Ashish, G. Chelliah, H. Parfrey, M. Thillai, J. Vila, S.V. Fletcher, P. Beirne, C. Favager, J. Brown, J. K. Dawson, P.R. Ortega, S. Haque, P. Watson, J.K. Khoo, K. Symons, P. Youssef, J. A. Mackintosh, Safety, tolerability, and efficacy of pirfenidone in patients with rheumatoid arthritis-associated interstitial lung disease: a randomised, double-blind, placebo-controlled, phase 2 study, Lancet Respir. Med. 11 (2023) 87–96, https://doi.org/10.1016/S2213-2600(22)00260-0.
[23] D. Gan, W. Cheng, L. Ke, A.R.J. Sun, Q. Jia, J. Chen, J. Lin, J. Li, Z. Xu, P. Zhang, Repurposing of pirfenidone (Anti-Pulmonary fibrosis drug) for treatment of rheumatoid arthritis, Front. Pharmacol. 12 (2021) 1–11, https://doi.org/10.3389/fphar.2021.631891.
[24] K.W. Lee, T.H. Everett, D. Rahmutula, J.M. Guerra, E. Wilson, C. Ding, J.E. Olgin, Pirfenidone prevents the development of a Vulnerable Substrate for Atrial fibrillation in a canine model of Heart Failure, Circulation 114 (2006) 1703–1712, https://doi.org/10.1161/CIRCULATIONAHA.106.624320.
[25] D.D. Chan, J. Li, W. Luo, D.N. Predescu, B.J. Cole, A. Plaas, Pirfenidone reduces subchondral bone loss and fibrosis after murine knee cartilage injury, J. Orthop. Res. 36 (2018) 365–376, https://doi.org/10.1002/jor.23635.
[26] J. Transl, Q. Wei, N. Kong, X. Liu, R. Tian, M. Jiao, Y. Li, H. Guan, K. Wang, Pirfenidone attenuates synovial fibrosis and postpones the progression of osteoarthritis by anti - fibrotic and anti - inflammatory properties in vivo and in vitro, J. Transl. Med. (2021) 1–12, https://doi.org/10.1186/s12967-021-02823-4.
[27] P.W. Noble, C. Albera, W.Z. Bradford, U. Costabel, M.K. Glassberg, D. Kardatzke, T. E. King, L. Lancaster, S.A. Sahn, J. Szwarcberg, D. Valeyre, R.M. Du Bois, Pirfenidone in patients with idiopathic pulmonary fibrosis (CAPACITY): two randomised trials, Lancet 377 (2011) 1760–1769, https://doi.org/10.1016/S0140-6736(11)60405-4.
[28] G.A. Margaritopoulos, A. Trachalaki, A.U. Wells, E. Vasarmidi, E. Bibaki, G. Papastratigakis, S. Detorakis, N. Tzanakis, K.M. Antoniou, Pirfenidone improves survival in IPF: results from a real-life study, BMC Pulm. Med. 18 (2018) 1–7, https://doi.org/10.1186/s12890-018-0736-z.
[29] D.J. Hines, D.L. Kaplan, Poly(lactic-co-glycolic) acid-controlled-release systems: experimental and modeling insights, Crit. Rev. Ther. Drug Carrier Syst. 30 (2013) 257–276, https://doi.org/10.1615/CritRevTherDrugCarrierSyst.2013006475.
[30] Y. Lei, Q. Zhang, G. Kuang, X. Wang, Q. Fan, F. Ye, Functional biomaterials for osteoarthritis treatment: from research to application, Smart Med 1 (2022) 1–14, https://doi.org/10.1002/smmd.20220014.
[31] M. Cao, M.T.Y. Ong, P.S.H. Yung, R.S. Tuan, Y. Jiang, Role of synovial lymphatic function in osteoarthritis, Osteoarthr. Cartil. 30 (2022) 1186–1197, https://doi.org/10.1016/j.joca.2022.04.003.
[32] M.D. Roman, R.S. Fleaca, A. Boicean, D. Bratu, V. Birlutiu, L.L. Rus, C. Tantar, S. I. Cernusca Mitariu, Assesment of synovial fluid pH in osteoarthritis of the HIP and knee, Rev. Chim. 68 (2017) 1242–1244, https://doi.org/10.37358/RC.17.6.5649.
[33] T. Noda, T. Okuda, R. Mizuno, T. Ozeki, H. Okamoto, Two-step sustained-release plga/hyaluronic acid gel formulation for intra-articular administration, Biol. Pharm. Bull. 41 (2018) 937–943, https://doi.org/10.1248/bpb.b18-00091.
[34] E.H. Lakes, K.D. Allen, Gait analysis methods for rodent models of arthritic disorders: reviews and recommendations, Osteoarthr. Cartil. 24 (2016) 1837–1849, https://doi.org/10.1016/j.joca.2016.03.008.
[35] H. Chen, G. Shen, Q. Shang, P. Zhang, D. Yu, X. Yu, Z. Zhang, W. Zhao, Z. Wu, F. Tang, D. Liang, X. Jiang, H. Ren, Plastrum testudinis extract suppresses osteoclast differentiation via the NF-κB signaling pathway and ameliorates senile osteoporosis, J. Ethnopharmacol. 276 (2021) 114195, https://doi.org/10.1016/j.jep.2021.114195.
[36] P. Kaukinen, J. Podlipská, A. Guermazi, J. Niinimäki, P. Lehenkari, F.W. Roemer, M.T. Nieminen, J.M. Koski, J.P.A. Arokoski, S. Saarakkala, Associations between MRI-defined structural pathology and generalized and localized knee pain – the Oulu Knee Osteoarthritis study, Osteoarthr. Cartil. 24 (2016) 1565–1576, https://doi.org/10.1016/j.joca.2016.05.001.
[37] Y. Yazici, T.E. McAlindon, A. Gibofsky, N.E. Lane, C. Lattermann, N. Skrepnik, C. J. Swearingen, I. Simsek, H. Ghandehari, A. DiFrancesco, J. Gibbs, J.R.S. Tambiah, M.C. Hochberg, A Phase 2b randomized trial of lorecivivint, a novel intra-articular CLK2/DYRK1A inhibitor and Wnt pathway modulator for knee osteoarthritis, Osteoarthr. Cartil. 29 (2021) 654–666, https://doi.org/10.1016/j.joca.2021.02.004.
[38] F. Eckstein, J.L. Kraines, A. Aydemir, W. Wirth, S. Maschek, M.C. Hochberg, Intra-articular sprifermin reduces cartilage loss in addition to increasing cartilage gain independent of location in the femorotibial joint: post-hoc analysis of a randomised, placebo-controlled phase II clinical trial, Ann. Rheum. Dis. 79 (2020) 525–528, https://doi.org/10.1136/annrheumdis-2019-216453.
[39] Y. Yazici, T.E. McAlindon, A. Gibofsky, N.E. Lane, D. Clauw, M. Jones, J. Bergfeld, C.J. Swearingen, A. DiFrancesco, I. Simsek, J. Tambiah, M.C. Hochberg, Lorecivivint, a novel intraarticular CDC-like kinase 2 and dual-specificity tyrosine phosphorylation-regulated kinase 1A inhibitor and Wnt pathway modulator for the treatment of knee osteoarthritis: a phase II randomized trial, Arthritis Rheumatol. 72 (2020) 1694–1706, https://doi.org/10.1002/art.41315.
[40] X. Zhu, Y.T. Chan, P.S.H. Yung, R.S. Tuan, Y. Jiang, Subchondral bone remodeling: a therapeutic target for osteoarthritis, Front. Cell Dev. Biol. 8 (21) (2021) 607764, https://doi.org/10.3389/fcell.2020.607764.
[41] Y. Jiang, Osteoarthritis year in review 2021: biology, Osteoarthr, Cartil 30 (2022) 207–215, https://doi.org/10.1016/j.joca.2021.11.009.
[42] A. Aimo, G. Spitaleri, D. Nieri, L.M. Tavanti, C. Meschi, G. Panichella, J. Lupón, F. Pistelli, L. Carrozzi, A. Bayes-Genis, M. Emdin, Pirfenidone for idiopathic pulmonary fibrosis and beyond, card. Fail, Rev 8 (2022), https://doi.org/10.15420/cfr.2021.30.
[43] R. Fava, N. Olsen, J. Keski-Oja, H. Moses, T. Pincus, Active and latent forms of transforming growth factor beta activity in synovial effusions, J. Exp. Med. 169 (1989) 291–296, https://doi.org/10.1084/jem.169.1.291.
[44] T.E. King, W.Z. Bradford, S. Castro-Bernardini, E.A. Fagan, I. Glaspole, M. K. Glassberg, E. Gorina, P.M. Hopkins, D. Kardatzke, L. Lancaster, D.J. Lederer, S. D. Nathan, C.A. Pereira, S.A. Sahn, R. Sussman, J.J. Swigris, P.W. Noble, A phase 3 trial of pirfenidone in patients with idiopathic pulmonary fibrosis, N. Engl. J. Med. 370 (2014) 2083–2092, https://doi.org/10.1056/nejmoa1402582.
[45] P.W. Noble, C. Albera, W.Z. Bradford, U. Costabel, M.K. Glassberg, D. Kardatzke, T. E.K. Jr, L. Lancaster, Pirfenidone in patients with idiopathic pulmonary fi brosis (CAPACITY): two randomised trials, Lancet 377 (2011) 1760–1769, https://doi.org/10.1016/S0140-6736(11)60405-4.
[46] I. Glaspole, D. Ph, M.K. Glassberg, E. Gorina, P.M. Hopkins, D. Kardatzke, D. Ph, L. Lancaster, D.J. Lederer, S.D. Nathan, C.A. Pereira, S.A. Sahn, R. Sussman, J. J. Swigris, P.W. Noble, A. Study, A Phase 3 Trial of Pirfenidone in Patients with Idiopathic Pulmonary Fibrosis (2022) 2083–2092, https://doi.org/10.1056/NEJMoa1402582.
[47] L. Chen, J. Zhang, J. Wang, J. Lin, X. Luo, W. Cui, Inflammation-regulated auto aggregated hydrogel microspheres via anchoring cartilage deep matrix for genes delivery, Adv. Funct. Mater. 33 (2023) 1–13, https://doi.org/10.1002/adfm.202305635.
[48] F. Lin, Y. Li, W. Cui, Injectable hydrogel microspheres in cartilage repair, Biomed, Technol. 1 (2023) 18–29, https://doi.org/10.1016/j.bmt.2022.11.002.
[49] M. Lu, X. Zhang, Z. Luo, Y. Zhao, Developing hierarchical microneedles for biomedical applications, Eng. Regen. 4 (2023) 316–327, https://doi.org/10.1016/j.engreg.2023.04.004.
[50] D.A. Binks, E.M. Gravallese, D. Bergin, R.J. Hodgson, A.L. Tan, M.M. Matzelle, D. McGonagle, A. Radjenovic, Role of vascular channels as a novel mechanism for subchondral bone damage at cruciate ligament entheses in osteoarthritis and inflammatory arthritis, Ann. Rheum. Dis. 74 (2015) 196–203, https://doi.org/10.1136/annrheumdis-2013-203972.
[51] X. Li, X. Li, J. Yang, Y. Du, L. Chen, G. Zhao, T. Ye, Y. Zhu, X. Xu, L. Deng, W. Cui, In situ sustained macrophage-targeted nanomicelle–hydrogel microspheres for inhibiting osteoarthritis, Research 6 (2023), https://doi.org/10.34133/research.0131.
[52] H. Nakazato, H. Oku, S. Yamane, Y. Tsuruta, R. Suzuki, A novel anti-fibrotic agent pirfenidone suppresses tumor necrosis factor-α at the translational level, Eur. J. Pharmacol. 446 (2002) 177–185, https://doi.org/10.1016/S0014-2999(02)01758-2.
[53] H.P. Benton, A. V Esquivel, A.D. Rice, S.N. Giri, Modulation of articular chondrocyte activity by pirfenidone, Res. Commun. Mol. Pathol. Pharmacol. 113–114 (2003) 275–288. http://www.ncbi.nlm.nih.gov/pubmed/15686126.
[54] H.S. Hwang, I.Y. Park, J.I. Hong, J.R. Kim, H.A. Kim, Comparison of joint degeneration and pain in male and female mice in DMM model of osteoarthritis, Osteoarthr. Cartil. 29 (2021) 728–738, https://doi.org/10.1016/j.joca.2021.02.007.